

# Nanoscale

Accepted Manuscript

This article can be cited before page numbers have been issued, to do this please use: X. Hu, D. Guo and N. T. K. Thanh, *Nanoscale*, 2026, DOI: 10.1039/D5NR04488J.



This is an Accepted Manuscript, which has been through the Royal Society of Chemistry peer review process and has been accepted for publication.

Accepted Manuscripts are published online shortly after acceptance, before technical editing, formatting and proof reading. Using this free service, authors can make their results available to the community, in citable form, before we publish the edited article. We will replace this Accepted Manuscript with the edited and formatted Advance Article as soon as it is available.

You can find more information about Accepted Manuscripts in the [Information for Authors](#).

Please note that technical editing may introduce minor changes to the text and/or graphics, which may alter content. The journal's standard [Terms & Conditions](#) and the [Ethical guidelines](#) still apply. In no event shall the Royal Society of Chemistry be held responsible for any errors or omissions in this Accepted Manuscript or any consequences arising from the use of any information it contains.

## ARTICLE

**Ion interference and its combined therapies for cancer treatments**Xinkai Hu,<sup>#a,b</sup> Dongdong Guo<sup>#a,b</sup> and Nguyen Thi Kim Thanh<sup>\*a,b</sup>Received 00th January 20xx,  
Accepted 00th January 20xx

DOI: 10.1039/x0xx00000x

Despite continuous advances in oncology, there remains a pressing need for tumour-specific therapies that can adapt to the unique tumour microenvironment while maintaining high efficacy and low systemic toxicity. Inspired by the critical role of ionic homeostasis in cancer cell survival, ion interference therapy has emerged as a strategy that exploits intracellular ions as cytotoxic effectors to selectively disrupt tumour viability. In particular, nano-engineered platforms enable precise manipulation of ion fluxes through ion-releasing nanomaterials, artificial nanochannels, and transporter-modulating systems, and can be readily integrated with conventional therapeutic modalities. By responding to specific tumour microenvironment and metabolic imbalances, nano-enabled ion interference offers spatially confined and stimulus-responsive cytotoxicity, providing a promising framework for precision nanomedicine.

**1. Introduction**

A wide range of tumour treatments have been developed, including the development of new oncology drugs and research into new therapies. Current cancer therapies using nanotechnology include chemodynamic therapy (CDT),<sup>1</sup> photodynamic therapy (PDT),<sup>2</sup> photothermal therapy (PTT),<sup>3</sup> sonodynamic therapy (SDT)<sup>4</sup> and imaging-assisted therapies.<sup>5</sup> Although there have been many reviews that have summarized these therapies, there is a lack of presentation on the roles and mechanisms of the therapeutic influence of ions presented. In fact, these therapies may be triggered by small molecule drugs, macromolecular polymers or ions. We believe that a classification of the “initiators” of these therapies will help us to clearly understand the advantages and disadvantages of using various substances to initiate CDT, PDT, PTT, and SDT. From an ionic perspective, we have summarized the most recent advances in ion-initiated therapies.

The development of nanotechnology has significantly expanded the possibilities for ion-based tumour therapy. Nanoscale materials can accumulate in tumours, enter cells more efficiently,<sup>6</sup> and release ions in a more controlled manner compared with bulk materials. Their surface properties and structural tunability also allow them to respond to tumour-specific conditions such as acidity or redox imbalance. In this way, nanomaterials serve not only as delivery vehicles, but also as active platforms for modulating ionic homeostasis.<sup>7</sup> Viewing ion interference through the lens of nanoscale engineering

therefore helps to better understand both its mechanistic basis and its therapeutic potential.

In addition to endless arrays of proteins, nucleic acids and other biomolecules contained within cells, ions also play a part in sustaining biological activity. A wide variety of ions perform a diverse range of roles within the cell, including maintaining osmotic pressure, participating in cell signalling, engaging in intracellular chemical reactions and acting as structural substances. Based on these aspects, therapies have been developed which are collectively known as ion-based therapies. These therapies regulating intracellular ion osmolarity (using ion flux or controlling ion channels), interfering with the signalling pathways, disrupting the balance of intracellular chemical reactions, or triggering CDT, PDT etc., can be very effective in treating tumours. Ion interference therapy is one of the homeostatic strategies used to treat disease, while the regulation of homeostasis also involves metabolic interference, redox regulation and cellular interactions, which are interrelated, but each has its own strengths.<sup>8</sup> Here, ion interference refers to therapeutic strategies that disturb ionic homeostasis in tumour cells. This can occur through specific mechanisms, such as regulating ion channels or transporters, or through less specific processes, including membrane disruption, ion leakage and interfacial ion redistribution.<sup>9,10</sup> Some systems also function by releasing ions intracellularly or triggering ion-dependent reactions, which further amplify ionic imbalance and cell damage. The ion therapies readily utilize the intratumoural environment and substances within the cell itself to produce a reasonable stimulation of tumour cells, which exhibits significant anti-tumour activity while avoiding general toxicity. Based on these ideas, some groups have developed CDT-enhanced tumour therapies using Fe<sup>2+</sup>, Mn<sup>2+</sup> and Cu<sup>2+</sup> ions,<sup>11-16</sup> all with good experimental results; others have attempted to alter intracellular Ca<sup>2+</sup>, Zn<sup>2+</sup> and H<sup>+</sup>,<sup>17-21</sup> some by directly increasing intracellular ion concentrations through nanoparticles (NPs) and others by modulating cellular ion

<sup>a</sup> Biophysics Group, Department of Physics and Astronomy, University College London, UK

<sup>b</sup> UCL Healthcare Biomagnetics and Nanomaterials Laboratories, The Royal Institution, 21 Albemarle Street, London, W1S 4BS, UK.

\*E-mail: [ntk.thanh@ucl.ac.uk](mailto:ntk.thanh@ucl.ac.uk)

<sup>#</sup>Contributed equally to this work



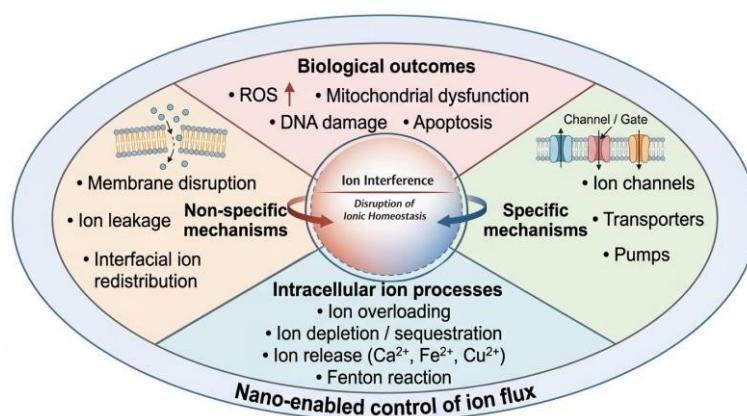


**Figure 1** Mechanism-based framework of ion interference in tumour therapy. Ion interference disrupts intracellular ionic homeostasis through non-specific mechanisms (e.g., membrane disruption and ion leakage) and specific mechanisms (e.g., modulation of ion channels and transporters). Intracellular ion processes, including ion overloading, depletion, and release, further amplify ionic imbalance. Ion-mediated reactions such as Fenton chemistry generate reactive oxygen species (ROS), ultimately leading to mitochondrial dysfunction, DNA damage, and apoptosis. Nanoscale systems enable controlled ion modulation and improve therapeutic outcomes.



**Xinkai Hu**

Xinkai Hu received his Master of Research (MRes) in Nanomaterials with Distinction from Imperial College London in 2021. During his integrated master's programme, he conducted research on the synthesis and characterization of anti-inflammatory nano polymers for targeted drug delivery applications. His research interests lie at the intersection of nanomedicine, medicinal chemistry, and smart drug

delivery systems. He is currently a PhD student at University College London (UCL) in Biophysics Group, the Department of Physics & Astronomy under the supervision of Prof. Nguyen Thi Kim Thanh and Dr Martin Forster. His doctoral research is dedicated to developing a heat-responsive magnetic drug delivery system based on iron oxide nanoflowers encapsulated in thermosensitive lipid vesicles, enabling combined magnetic hyperthermia and chemotherapy for the treatment of head and neck cancer. His work integrates nanoscale material design, liposome delivery system and 3D tumour model studies, aiming to advance translational cancer nanomedicine from fundamental mechanisms toward therapeutic applications.



**Dongdong Guo**

Dongdong Guo received his MSc degree in Chemistry from Tsinghua University, Beijing, in 2021. He is currently pursuing his PhD under the supervision of Prof. Nguyen Thi Kim Thanh at University College London (UCL). His research interests focus on the development of nanomaterials for cancer theranostic and on elucidating the molecular mechanisms of heating-nanomaterial-induced cell damage.



**Nguyen Thi Kim Thanh**

Professor Nguyen Thi Kim Thanh, MAE, FRSC, FInstP, FAPS, FIMMM FRSB (<https://www.ntk-thanh.co.uk>) held a prestigious Royal Society University Research Fellowship (2005–2014). She was appointed a Full Professor in Nanomaterials in 2013 at University College London. She leads a very dynamic group conducting cutting-edge interdisciplinary and innovative

research on the design and synthesis of magnetic and plasmonic nanomaterials, mainly for biomedical applications. In 2019, she was honoured for her achievements in the field of nanomaterials and was awarded the highly prestigious Royal Society Rosalind Franklin Medal. She was RSC Interdisciplinary Prize winner in 2022. She was awarded SCI/RSC Colloids Groups 2023 Graham Prize Lectureship to recognise an outstanding mid-career researcher in colloid and interface science. She is one of 12 recipients globally of 2023 Distinguished Women in Chemistry/Chemical Engineering Awards, bestowed by the International Union of Pure and Applied Chemistry (IUPAC). She was Vice Dean for Innovation and Enterprise at the Faculty of Maths and Physical Sciences. She was elected as a member of Academia Europaea in April 2024. She is Editor-in chief of the Royal Society of Chemistry book Series, Nanoscience and Nanotechnology and an Associate Editor for Nanoscale and Nanoscale Advances Journals. She edited 9 theme issues including: *Magnetic Nanoparticles: From Massart Method to a Cascade of Innovations 2026*; *Design and scaling up of theranostic nanoplatfoms for health: towards translational studies*. *Nanoscale*, RSC (2023); *Theranostic nanoplatfoms for biomedicine* *Nanoscale*, RSC (2021). She is the sole editor of two seminal books on *Magnetic Nanoparticles from Fabrication to Clinical Applications* (<https://tinyurl.com/y5bgxb3r>) and *Clinical Applications of Magnetic nanoparticles* (<https://tinyurl.com/yyjawnz2>)



transport proteins. In this review, we look at the ions themselves, review the ion interference technologies that have been developed to date, highlight some of the tumour treatment strategies that are promising and the difficulties that remain, and conclude with an outlook on possible new applications or strategies that may emerge in the future.

## 2. Ion interference as primary therapy

As summarised in Figure 1, ion interference therapies are designed to disrupt intracellular ionic homeostasis, thereby inducing tumour cell dysfunction or death. Mechanistically, these approaches can be categorised into three main modes: (i) direct modulation of intracellular ion levels, (ii) non-specific processes such as membrane disruption and ion leakage, and (iii) specific regulation of ion flux via ion channels, transporters, or pumps. These mechanisms collectively lead to a range of biological outcomes, including oxidative stress, mitochondrial dysfunction, DNA damage, and apoptosis.

### 2.1. Regulating intracellular ion levels

Various ions present in the cell maintain a dynamic equilibrium process while assuming unique and important roles, and that is a macroscopic manifestation of intracellular ionic homeostasis. Typically, taking the ions  $\text{Na}^+$ ,  $\text{K}^+$ , and  $\text{Cl}^-$  as examples, they maintain a stable concentration gradient inside and outside the cell, and it is this concentration gradient that plays a crucial role in maintaining the cytoskeletal structure and physiological processes.<sup>22-24</sup> This is due to the fact that, from our current knowledge,  $\text{Na}^+$ ,  $\text{K}^+$ , and  $\text{Cl}^-$  are key ions in the regulation of cellular osmolarity.<sup>25</sup> When the balance of these ions in and around cells is disrupted, for example, the disturbance of the cytoskeleton, cell cycle arrest, or even cell lysis and death could result from the imbalance of the osmotic pressure between the interior and exterior of cells.<sup>26, 27</sup> Some intracellular ions, such as  $\text{Ca}^{2+}$  and the trace elements  $\text{Zn}^{2+}$  and  $\text{Cu}^{2+}$ , are also in dynamic equilibrium (homeostasis) within the cell as well as in the tissues. Deviations from the normal intracellular concentration thresholds of  $\text{Ca}^{2+}$ ,  $\text{Zn}^{2+}$  and  $\text{Cu}^{2+}$  can disrupt key physiological processes. Whether these ions increase or decrease beyond their normal ranges, such imbalance may affect cellular signalling, chromosome replication,<sup>28</sup> and osmotic homeostasis. In the next section, we discuss therapeutic strategies that exploit these ion-dependent processes as targets.

#### 2.1.1. Ion overloading strategies

The intracellular homeostasis of ions is not only related directly to various ions per se, such as  $\text{Na}^+$ ,  $\text{K}^+$ ,  $\text{Cl}^-$ , and  $\text{Ca}^{2+}$ , but also indirectly to the ion channels or ion transporters. Hence, the methods of artificial intervention in intracellular ion homeostasis can be divided into direct and indirect interventions. Direct intervention is the “insertion” of a target ion into the cell by means of drug delivery, thereby disrupting the intended intracellular homeostasis of the ion and consequently causing cell lysis. This means of forcing the target ions into the cell is until it overloaded. Zhu et al. in 2012 reported the use of nanodiamonds (NDs) to deliver large amounts of  $\text{Na}^+$  into cells, which successfully induced

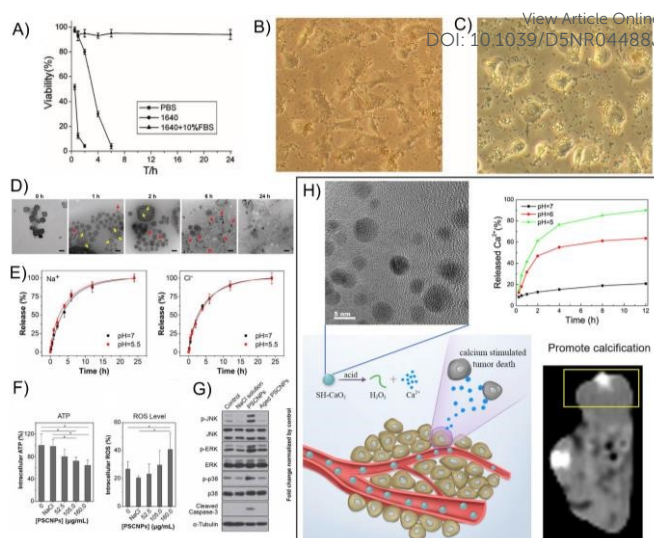


**Figure 2** Nanomaterial-enabled ion overloading strategies for therapeutic intervention. (A) Cell viability of HeLa cells after incubation with nanodiamonds (NDs) in phosphate buffered saline (PBS), RPMI-1640, and complete culture medium, indicating medium-dependent cytotoxicity. (B, C) Optical microscopy images of HeLa cells after 2 h incubation with NDs in cell culture media (B) and PBS (C). (A-C) Reproduced with permission.<sup>29</sup> Copyright 2012, Wiley-VCH GmbH. (D) Transmission electron microscopy (TEM) images showing the progressive degradation of phospholipid coated NaCl nanoparticles (PSCNPs) in water over 24 h, with surface cavity formation (yellow arrows), fragmentation (red arrows), and complete dissolution. (E)  $\text{Na}^+$  and  $\text{Cl}^-$  ion release profiles from PSCNPs in ammonium acetate buffers at pH 7.0 and 5.5, monitored by  $\text{Na}^+$ -selective electrode and MQAE fluorescence. (F) Intracellular adenosine triphosphate (ATP) depletion and reactive oxygen species (ROS) elevation after 6 h treatment with increasing PSCNP concentrations (\* $p < 0.05$ ). (G) Western blot analysis of mitogen-activated protein kinase (MAPK) signalling [c-Jun NH 2-terminal kinase (JNK), extracellular signal-regulated kinase (ERK), and p38] in PC-3 cells treated with PSCNPs ( $160 \mu\text{g mL}^{-1}$ ), compared with PBS, NaCl, and pre-degraded PSCNP controls. (D-G) Reproduced with permission from.<sup>35</sup> Copyright 2019, Wiley-VCH GmbH. (H) Schematic showing the function of SH- $\text{CaO}_2$  NPs in acidic tumour environments: decomposition into  $\text{Ca}^{2+}$  and  $\text{H}_2\text{O}_2$  leads to calcium overload and ROS accumulation, triggering cancer cell death and potential tumour calcification. Reproduced with permission.<sup>37</sup> Copyright 2019, Elsevier.

intracellular osmotic pressure and a subsequent series of intracellular oxidative stress responses, demonstrating good tumour therapeutic effects (Figure 2A-C).<sup>29</sup> Here, they used nano-diamonds as an adsorbable “sponge” to successfully target the release of excessive  $\text{Na}^+$  into tumour cells, causing cell swelling and ultimately cell destruction. This cleverly designed work illustrates for the first time how to implement a strategy for the rapid accumulation of intracellular ions to “kill” cells and its feasibility. This work provides an opportunity to overcome a barrier to ion delivery, namely the principle of electroneutrality, which has previously confused how to “cram” highly charged ions into cells.<sup>30, 31</sup> Similarly, some metal ions have been reported to be adsorbed by NDs, and the same group developed NDs- $\text{Cu}^{2+}$  complexes in 2015 and demonstrated potent tumour cytotoxicity by releasing  $\text{Cu}^{2+}$  upon acidic stimulation of lysosomes.<sup>32</sup> Although other ions have not been biologically validated, this approach does represent an effective means of inserting ions into cells. In fact, this method of ion delivery, in which the entire delivery process takes place in ion form, is technically difficult because the charged material is more likely to attach to proteins during circulation and form a protein corona, or to be bound to other ions or molecules of



opposite charge, leading to the failure of the ion targeting.<sup>33, 34</sup> It is often easier to adopt a “pro-drug” strategy for delivery, as the nanosystem remains in a non-ionic state until it enters the cell, making it much less likely to be removed or rejected and reducing the difficulty of delivering the drug to the destination. In contrast, the delivery process of pro-drug strategy is smoother, but this is accompanied by the requirement for a more refined design of the material structure, in terms of 1) a suitable substrate for ion release, 2) an optimized response mode, 3) a refined toxicity of the material's system, etc., while delivery efficiency and therapeutic efficacy are also under consideration for evaluation. In this scenario, Xie's group prepared a phospholipid coated NaCl NPs (PSCNPs),<sup>35</sup> a common electrolyte that has rarely been previously developed for tumour therapy without taking ion homeostasis strategies into account (Figure 2D). The reported NPs bypass ion regulatory and transport proteins before entering the cell and rapidly dissolving, causing a surge in osmotic pressure and subsequent cell lysis. Intriguingly, and thanks to the relatively low levels of sodium in normal cells, the group found that PSCNPs avoided serious damage to them. By using a seahorse mitochondrial stress assay on PSCNPs-treated cells, the researchers examined changes in mitochondrial oxygen consumption and respiration rates and found that both were reduced to 47.9% and 91.0%, respectively, which also decreased intracellular adenosine triphosphate (ATP) production and increased phosphorylation levels of c-Jun NH 2-terminal kinase (JNK), extracellular signal-regulated kinase (ERK), and p38, shown as Figure 2F-G. Thus, it was found that the abrupt imbalance of intracellular ions was not only related to osmotic pressure but also profoundly affected cellular metabolism and expression levels of proteins involved in several pathways, such as pyroptosis and apoptosis. Similarly, work on intracellular delivery of ions using compounds as prodrugs has also focused in the last two years on ion-disrupting therapies using calcium-related compounds. Because  $\text{Ca}^{2+}$  is ubiquitous in cells and mediates many important physiological processes, from cell proliferation to cell death,<sup>36</sup> it is of great interest to develop tumour therapies based around  $\text{Ca}^{2+}$ , so-called “calcium overload therapies”, which exploit the rapid accumulation of calcium ions in cells to kill tumours. In 2019, the Bu group first explored calcium accumulation-mediated tumour therapies, using calcium peroxide ( $\text{CaO}_2$ ) NPs to react with the  $\text{H}^+$  in the acidic environment of the tumour to generate  $\text{Ca}^{2+}$  and  $\text{H}_2\text{O}_2$ , thereby inducing simultaneous  $\text{Ca}^{2+}$  overload and oxidative stress.<sup>37</sup> Compared with microscale counterparts, nanoscale  $\text{CaO}_2$  enables improved tumour accumulation, enhanced cellular internalization, and more controllable intracellular ion release, thereby facilitating localized therapeutic effects and reducing off-target toxicity. The synthesized pH-sensitive sodium-hyaluronate-modified calcium peroxide (SH- $\text{CaO}_2$ ) NPs can initiate calcification and reactive oxygen species (ROS) burst in cells, as shown in Figure 2H. In this work, the choice of  $\text{CaO}_2$  as a substrate material is a wise idea. Since  $\text{CaO}_2$  not only rapidly responds to the acidic tumour (pH 5.0) microenvironment but also provides  $\text{Ca}^{2+}$  plus  $\text{H}_2\text{O}_2$  simultaneously, it is a very concise and effective nanosystem.

Several independent groups have subsequently developed nano-delivery systems using  $\text{CaO}_2$  as a carrier.<sup>38-40</sup> Most of these nanosystems enable the self-supply of  $\text{H}_2\text{O}_2$  and the sustained release of ROS, and combine ion overload therapy with PTT, PDT and acoustic therapy to achieve enhanced effects in multi-modal therapy. Similar calcium overload strategies were carried out by Chen et al.,<sup>41</sup> Pan et al.,<sup>42</sup> Li et al.<sup>43</sup> and Wang et al.<sup>44</sup> to treat cancers based on different carriers, such as  $\text{CaCl}_2$ , CaP,  $\text{CaCO}_3$ , and aminocyclopropane-1-carboxylic acid (ACC), with good therapeutic results. However, it is evident that  $\text{CaO}_2$  is preferred by researchers as a delivery pro-drug for  $\text{Ca}^{2+}$  interference therapy.<sup>45-48</sup> These approaches suggest promising applications for  $\text{Ca}^{2+}$  related ion therapies. Also in the Bu group, they constructed an up-conversion nanoparticle (UCNP@MIL-88B@PA) that can transiently boost  $\text{H}^+$  in tumour cells in order to enhance CDT and anti-metastasis.<sup>17</sup> In addition,  $\text{Zn}^{2+}$  and  $\text{Cu}^{2+}$  can have similar effects in exacerbating ion disorders and oxidative stress in cells.<sup>49</sup> And the Zn-based and Cu-based NPs,

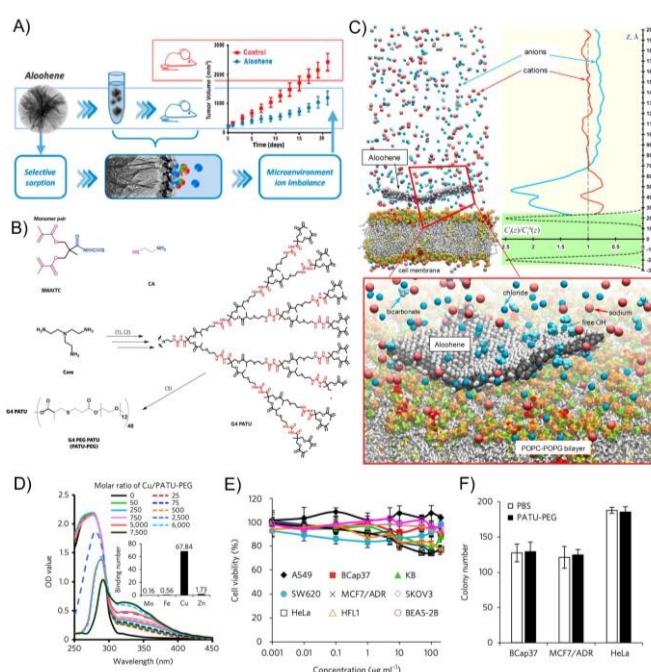


**Figure 3 Ion sequestration and redistribution strategies for disrupting tumour cell viability.** (A) Molecular dynamics simulation showing ion redistribution near the cell membrane induced by crumpled  $\text{Al}(\text{OH})_3$  nanosheets (Aloohene). Cations and anions exhibit distinct spatial distributions in the extracellular region adjacent to the Aloohene domain. (B) Concentration profile  $C_i(z)$  of cations (red) and anions (blue) as a function of distance  $z$  from the cell membrane, relative to their unperturbed levels  $C_{i0}(z)$ . Inset illustrates a magnified segment of the Aloohene-membrane interface with detailed colour coding for membrane and Aloohene components. (A, B) Reproduced with permission.<sup>9</sup> Copyright 2018, American Chemical Society. (C) Synthesis scheme of PEGylated fourth-generation PATU dendrimer (PATU-PEG) from BMAITC and CA. Only one dendron arm is shown; key synthetic steps are indicated (1-3). (D) Ultraviolet-visible spectra of PATU-PEG (10  $\mu\text{M}$ ) in the presence of varying concentrations of  $\text{CuCl}_2$ , after subtracting unbound  $\text{CuCl}_2$  absorbance. Inset shows high copper selectivity of PATU-PEG over other trace metals ( $\text{Mn}^{2+}$ ,  $\text{Fe}^{2+}$ ,  $\text{Zn}^{2+}$ ) at 20  $\mu\text{M}$  concentration, each metal at 20 mM. (E) Cytotoxicity of PATU-PEG in different cancer cell lines after 48 h treatment, assessed via 3-(4,5-dimethylthiazol-2-yl)-2,5-diphenyltetrazolium bromide (MTT) assay. (F) Colony formation assay showing reduced clonogenic survival after 10 d culture with PATU-PEG (200  $\mu\text{g mL}^{-1}$ ); colonies with more than 50 cells were counted. (C-F) Reproduced with permission.<sup>61</sup> Copyright 2018, Springer Nature.



in the form of ZnO,<sup>50</sup> ZnO<sub>2</sub>,<sup>51</sup> and Cu<sup>2+</sup>,<sup>15</sup> Cu-complexes,<sup>52</sup> have been developed to act as a modulator of intracellular Zn<sup>2+</sup> or Cu<sup>2+</sup> and as an initiator of oxidative stress. These works either use ion overloading or cause redox imbalance to force cell destruction.<sup>53-55</sup> Predictably, to our knowledge, although no current work on K<sup>+</sup> overload has been reported, K<sup>+</sup> has the same potential as Na<sup>+</sup>, Cl<sup>-</sup>, and Ca<sup>2+</sup> as an entry point for the development of new therapeutics due to its equal importance as Ca<sup>2+</sup> in maintaining intracellular osmolarity and other physiological functions.<sup>56</sup>

### 2.1.2. Ion sequestration or depletion strategies

Chelator-based approaches can regulate intracellular ion availability by sequestering or redistributing specific ions, which has been explored in clinically relevant contexts.<sup>57</sup> In addition to chelation, ionic homeostasis can also be disrupted through adsorption or immobilisation processes, in which target ions are captured or complexed and thereby prevented from functioning in their free ionic forms. Most of these methods lead to changes in the structure and morphology of the cell, which seems easier to understand when you think of it as pumping the gas out of a balloon until it dries up. Lerner et al.<sup>9</sup> reported in 2018 that a crumpled aluminium hydroxide nanosheet (Aloohene) can selectively adsorb extracellular anions (e.g., Cl<sup>-</sup>), thereby inducing severe ionic imbalance (Figure 3A). The two-dimensional nanosheet morphology provides an exceptionally high surface area and extensive interfacial contact with the cellular membrane, which enhances electrostatic interactions and anion adsorption efficiency compared with bulk or particulate counterparts. Molecular simulations further supported that such ion redistribution disrupts membrane potential homeostasis and ultimately leads to cell death (Figure 3B). The tumour growth inhibitory ability of Aloohene was demonstrated in four cell lines, MCF-7, UM-SCC-14C, HeLa, and PyMT, presumably because Al<sup>3+</sup> promotes the production of intracellular ROS and the subsequent oxidative stress damage. Although the Cu<sup>2+</sup> overload strategy has been experimentally proven to have a favourable anti-tumour effect,<sup>58</sup> Cu<sup>2+</sup> deficiency may lead to neurological or haematological disorders, which then inhibit tumour growth to a large extent.<sup>59, 60</sup> In this context, Shao et al.<sup>61</sup> devised a novel dendrimer that has a strong affinity for Cu<sup>2+</sup> and thus immobilizes bioavailable copper to form a complex, which in turn has the effect of inhibiting angiogenesis and cell proliferation, as both of these impairments allow for a significant inhibition of tumour growth (Figure 3C-F). This also validates our view that deviations from normal values of intracellular ions, in whatever way, affect the physiological processes of tumour cells.

In terms of strategies to overload or exhaust intracellular ions, future work could go beyond the conventional thinking about carriers and develop supramolecular loading materials based on three-dimensional (3D) mesh structures. On the one hand, these 3D cross-link materials have a good loading capacity for drug molecules or metal ions and can achieve a continuous release of ions; on the other hand, due to their natural adsorption capacity, some 3D materials can be transformed into

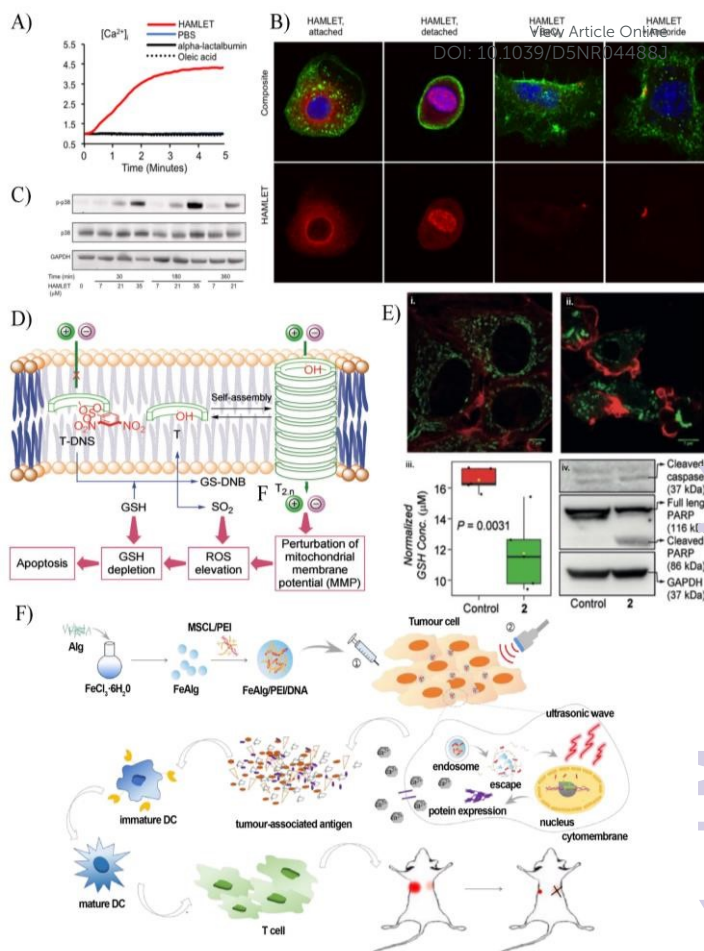


**Figure 4** Modulation of ion channels or transporters to disrupt cancer-associated signalling pathways. (A) Fluorescence-based quantification of intracellular Ca<sup>2+</sup> concentrations in A549 and Jurkat cells after treatment with HAMLET. Rapid and specific ion fluxes were observed, while control treatments ( $\alpha$ -lactalbumin, oleic acid, PBS) had no significant effects ( $n = 4$ ,  $*p < 0.05$ ). (B) Confocal microscopy images showing internalization of Alexa-568-labelled HAMLET (35  $\mu$ M, 1 h) into tumour cells. HAMLET localized peri-nuclearly and within nuclei. Internalization was inhibited by amiloride or BaCl<sub>2</sub>, leaving HAMLET at the membrane surface. Red: HAMLET; blue: nuclei (DraQ5); green: membranes (WGA); scale bar = 10  $\mu$ m. (C) Dose- and time-dependent activation of the p38 MAPK pathway in lung carcinoma cells treated with HAMLET. Phosphorylation was assessed by western blot and normalized to total p38 and GAPDH. (A-C) Reproduced under the terms of the CC-BY license.<sup>10</sup> Copyright 2013, Storm et al. (D) Schematic illustration of intracellular supramolecular channel formation. In the presence of intracellular GSH, monomer T is activated and assembles into T<sub>2-n</sub> supramolecular channels within the cell membrane. (E) Functional validation of a 2,4-nitrobenzenesulfonyl (DNS)-protected 2-hydroxyisophthalamide derivative (1.0  $\mu$ M). iii.) GSH levels were quantified in MCF-7 cells by <sup>1</sup>H NMR before and after treatment. Immunofluorescence staining of cytochrome c (green) shows its mitochondrial release upon ii.) treatment with compound (1.0  $\mu$ M), compared to i.) untreated cells. Phalloidin (red) was used for cell boundary staining. iv.) Immunoblot analysis further confirmed activation of the apoptotic pathway via detection of cleaved caspase-9 and cleaved/full-length PARP-1 after 24 h incubation. Statistical significance was assessed using Tukey's HSD test ( $*p < 0.05$ ,  $**p < 0.01$ ,  $***p < 0.001$ ). (D, E) Reproduced with permission.<sup>72</sup> Copyright 2020, Wiley-VCH GmbH. (F) Schematic of a sonogenetic nanosystem-based cancer immunotherapy. Iron alginate nanogel (FeAlg)/ polyethyleneimine (PEI)/ mechanosensitive ion channel of large (MSCL) hydrogel NPs were injected into primary tumours, enabling cellular uptake, endosomal escape, and MSCL plasmid release. After 48 h, MSCL ion channels were expressed, followed by local ultrasound triggering. Tumour cell apoptosis and debris release enhanced dendritic cell maturation and systemic immune responses, suppressing both primary and distant tumours. Reproduced with permission.<sup>74</sup> Copyright 2020, Elsevier.



ion adsorption “sponges” for the purpose of depleting intracellular ions, and these efforts are worth trying.

## 2.2. Modulating ion channels/transporters to interfere with signal transduction

In addition to biological ion channels, artificial ion channels have also been developed to modulate transmembrane ion flux, offering a synthetic approach to disrupt ionic homeostasis.<sup>62</sup> In contrast to strategies that directly alter intracellular ion concentrations, ion interference can also be achieved through the specific modulation of ion channels and transporters, which govern ion influx and efflux across cellular membranes.<sup>63</sup> It has been recognised since the 1980s that ion channels are closely associated with abnormal cell proliferation and are therefore strongly linked to tumour development.<sup>64</sup> Most notably,  $\text{Ca}^{2+}$  and  $\text{K}^+$  channels are known to regulate cell proliferation and apoptosis.<sup>65</sup> Ion channels are not only involved in the regulation of intracellular ion homeostasis and exchange but also have a role in initiating and participating in cellular signal regulation.<sup>24</sup> The various ion channels include voltage-gated channels, which are regulated by membrane potential to transport certain specific ions, and ligand-gated channels, which are regulated by ligand to transport some common ions.<sup>66</sup> Other reviews<sup>67-71</sup> have summarized in detail the relationship between these ion channels and tumours, from tumorigenesis to tumour progression to migration and invasion, and immune cell activation as well. To gain a better understanding of the important role that ion channels play in tumour development, we strongly recommend that readers refer to these well-rounded reviews. Today, various new approaches are also being developed for the regulation of ion channels in the hope of achieving tumour growth inhibition and, more promisingly, tumour cure. Considering that the ion channels or transporters that control ion influx and efflux are like the valves that control gas in and out a balloon, an indirect way to interfere with intracellular ion homeostasis is to interfere with the ion “valves” that are used to transport or regulate intracellular ion homeostasis thereby affecting the inward and outward flow of ions. Typically,  $\text{Na}^+$ ,  $\text{K}^+$ ,  $\text{Cl}^-$ , and  $\text{Ca}^{2+}$  channels are used as targets to further activate the immune response or directly kill tumour cells.

As highlighted in Figure 4A-C, Stor et al.<sup>10</sup> investigated human alpha-lactalbumin made lethal to tumour cells (HAMLET), which induced non-selective ion flow-induced tumour cell death, the main strategy of which was to induce rapid  $\text{Ca}^{2+}$  flow through over-activated ion channels, causing substantial disruption of various physiological processes within the tumour cells. In addition, exposure to HAMLET induces tumour cell morphology, transcriptomic alterations, and abnormal MAPK signalling. The HAMLET shows rapid membrane perturbation while activating a non-selective cation current. It is known that the rapid ion flow, both into and out of the cells, has a significant impact on the cells. On a more related level, a more interesting attempt was made by Talukdar's group (Figure 4D), who devised an artificial ion channel dependent on glutathione (GSH) activation that could release high levels of GSH to ion transporters and

thus cause apoptosis by disturbing the balance of anions and cations.<sup>72</sup> Changes in intracellular ions are accompanied by an increase in intracellular ROS and a decrease in GSH (Figure 4E i), as well as the release of cytochrome c caused by altered mitochondrial membrane permeability and PARP cleavage, which ultimately leads to the cell entering the apoptotic process (Figure 4E ii-iv). This work assessed the differences in cell viability induced by an intracellular imbalance between metal ion-related ( $\text{M}^+$ ) and  $\text{Cl}^-$ , suggesting that the approach to ion channel manipulation has a dramatic impact on a range of ion homeostasis within the cell. Similar work was demonstrated by Han et al.<sup>73</sup> in 2008 on ovarian tumour cells using the  $\text{K}^+$  opener NS1619, the involvement of which makes imbalance in  $\text{K}^+$  homeostasis an important indicator of tumour cell killing. As schematized in Figure 4F, He et al.<sup>74</sup> recently reported an ultrasound-responsive nanosystem that activates the mechanosensitive channel of large conductance (MSCL). This activation induces sustained intracellular  $\text{Ca}^{2+}$  accumulation, which subsequently triggers programmed apoptosis in tumour cells. Experimental results further showed that this strategy can enhance immune responses against tumours. This work is very similar to, but not identical to, the  $\text{Ca}^{2+}$  overload strategy described in the previous section; the former involves the direct delivery of  $\text{Ca}^{2+}$  or its precursors into the cell, whereas the latter involves the manipulation of ion channels to affect ion flow or intracellular ion reservoirs for the purpose of disrupting cellular physiological processes. Overall, a large body of work has shown that targeting ion channels through either small-molecule drugs or antibody molecules can also cause changes in ion flow to inhibit tumour growth.<sup>75-77</sup> There is no doubt that an increase or decrease in intracellular ions (by whatever means, direct or indirect) not only affects cellular osmolarity homeostasis but also causes changes in other physiological processes, such as signalling, as will be briefly discussed in the next section.

The relationship between ion channel proteins and intracellular ion homeostasis was mentioned in the previous section. Still, in fact, intracellular imbalance of these ions is only one of the results of interference with ion channels or transporters, which have been shown to be closely related to intracellular signalling. Ion channel interference, with certain signalling pathways, has become an effective tool in tumour therapy. The more important intracellular ion channel is those related to  $\text{Ca}^{2+}$  and  $\text{K}^+$  transport, which are involved in several signalling processes, such as  $\text{Ca}^{2+}$  signalling and cell cycle, which have been summarized in other reviews, and we refer the readers to the literature.<sup>78, 79</sup>

Thus, in summary, we can see that interfering with ion channel proteins has the dual effect on 1) intracellular ion homeostasis and osmotic pressure homeostasis and 2) intracellular signalling, and therefore therapeutic strategies that use ion channel as targets for tumour therapy are gradually receiving widespread attention and laying the foundation for their application in clinical treatment.

## 2.3. Ion-binding leads to altered DNA/protein function

Platinum ion ( $\text{Pt}^{2+}$ )-related compounds have been in clinical use for many years as broad-spectrum anticancer agents. In this



case, the therapeutic effect arises from direct interactions between metal ions and biomolecular targets, such as DNA or proteins, which represents another form of ion-mediated biological interference. The anti-cancer mechanism of platinum (Pt)-containing drugs is similar in that they all tend to bind to the guanine residue of DNA to form a Pt-DNA adduct, which then forms inter- or intra-molecular cross-links between DNA molecules, thereby disrupting the DNA double helix structure and impeding the polymerase process.<sup>80</sup> Based on this idea, the very first-line anti-cancer drug cisplatin has been developed. Specifically, the cisplatin molecule enters the cell and first undergoes a hydrolysis process to produce the highly active platinum complex  $[Pt(NH_3)_2ClH_2O]^+$ . This complex then binds to the N7 atom on the guanine or adenine residues of DNA. The remaining chloride ligand is then further hydrolysed to create a vacancy allowing Pt to bind to a second nucleotide base.<sup>81</sup> This thus makes the DNA double helix structure kinked. Conventional Pt-based chemotherapeutic agents, such as cisplatin, disrupt DNA replication and transcription mainly through the formation of covalent Pt-DNA adducts. However, these adducts are usually recognized and repaired by the nucleotide excision repair (NER) pathway, thus limiting efficacy. A new strategy has been proposed by researchers to combat Pt resistance by simultaneously exploiting the ion-binding ability and catalytic activity of Pt-based nano-enzymes. In Figure 5A, Li et al.<sup>82</sup> designed nuclease-mimetic platinum nanozymes (NMPNs) capable of inducing dual-mode DNA damage. These nanostructures not only form stable Pt-DNA adducts but also generate ROS in situ through their oxidase- and peroxidase-like activities. Importantly, this ROS production results in oxidative cleavage of DNA strands adjacent to the Pt binding sites, fundamentally altering the DNA conformation necessary for NER protein recruitment. This impairs DNA bending and blocks DNA repair, causing the adducts to persist and accumulate, ultimately leading to tumour cell apoptosis. In vivo studies demonstrated that NMPNs significantly suppressed tumour growth in mouse models, outperforming cisplatin in both efficacy and biosafety. Moreover,  $Pt^{2+}$  acts as both structural binders and biochemical effectors, anchoring DNA lesions while simultaneously disrupting repair pathways through oxidative cleavage. These nanozymes offer a promising path forward for overcoming the limitations of conventional DNA-targeting agents. The study demonstrates the potential of ion-driven therapy to progress beyond the limitations of passive drug delivery, thereby entering the domain of active biological modulation. There are many more similar systems for Pt delivery, which can be found in other literatures.<sup>83, 84</sup> However, despite Pt's indelible contribution to the history of the fight against cancer, it has to be pointed out that each of these Pt drugs is only effective against individual tumours and, because they are not tumour-specific, their use is associated with serious side effects. It has also been shown that Pt can bind not only to DNA but also to proteins. The formed Pt-protein complexes will no longer have a significant anti-cancer effect,<sup>85</sup> which is understandable as binding to proteins is only an interim, not a finale. In terms of Pt-based chemotherapy, the tumour activity can still be maintained if the DNA that encodes



**Figure 5 Ion binding induces changes in DNA/protein function through structural interference or signalling disruption.** (A) Schematic illustration of the synthesis and therapeutic mechanism of nuclease-mimetic platinum nanozymes (NMPNs). i) Pt nanoclusters (PtNCs) were sequentially modified with Polyethylene glycol (PEG) and trans-activator of transcription (TAT) peptides to produce NMPNs, enabling enhanced tumour targeting. Under mildly acidic conditions, TAT peptide exposure promotes the nuclear accumulation of NMPNs, where they induce DNA platination and in situ ROS generation. The oxidative cleavage of DNA disrupts the structural basis required for nucleotide excision repair (NER), preventing the recruitment of repair proteins such as xeroderma pigmentosum group A and F (XPA and XPF), thereby effectively inhibiting the NER pathway and enhancing therapeutic efficacy against platinum-resistant tumour cells. ii) Cell viability assays showed that NMPNs significantly reduced the survival of cisplatin-resistant Huh7 cells ( $n = 4$  independent experiments). iii) Representative bioluminescence imaging confirmed superior tumour inhibition in the NMPN-treated group compared with controls, cisplatin, and Pt NPs across multiple time points. Reproduced under the terms of the CC-BY license.<sup>82</sup> Copyright 2022, Li et al. (B) Characterization and biological evaluation of AgNPs in triple-negative breast cancer (TNBC) and non-malignant breast epithelial cells (MCF-10A). i) TEM imaging confirmed the uniform size and morphology of AgNPs. ii) The cytotoxic effects of AgNPs and silver ions ( $AgNO_3$ ) were assessed by MTT assay after 48 h exposure, showing a concentration-dependent reduction in cell viability in MDA-MB-231 cells, while MCF-10A cells remained largely unaffected. iii) Further MTT analysis after 24 h treatment demonstrated selective toxicity of AgNPs toward TNBC cells over non-malignant cells. iv) Confocal microscopy of 3D cultured S1 acini revealed that AgNP treatment did not significantly disrupt tight junction integrity, as indicated by ZO-1 staining. v) DNA damage quantification by 53BP1 immunostaining showed a dose-dependent increase in DNA damage foci in MDA-MB-231 cells treated with AgNPs, comparable to the damage induced by ionizing radiation (3 Gy), confirming that AgNPs promote genotoxic stress in cancer cells without severely affecting non-malignant cells. Scale bars = 10  $\mu m$ . Reproduced under the terms of the CC-BY license.<sup>88</sup> Copyright 2019, Swanner et al.



the tumour-related protein has not been directly targeted. In this way we can understand the significance of using nanosystems to deliver Pt drugs, 1) to refine their targeting capability and reduce side effects; 2) to reduce their loss in circulation and increase their efficacy; and more crucially 3.) to use nanosystems to assist in providing an important practical basis for their combination with other therapies. Based on the above, in recent years, there have been several attempts to find other ions to replace Pt-containing drugs in tumour therapy. Silver NPs have thus been found to be of substantial exploratory value. Some silver complexes have also succeeded in attracting attention due to their lower side effects compared to Pt, their higher activity, and the fact that they are less likely to become drug resistant. The anticancer activity of Ag<sup>+</sup> is mainly due to interference with topoisomerases, and some studies have shown that silver complexes have more potent anticancer properties than 5Fu and exhibit low toxicity to other cells; other silver compounds interfere with DNA replication by inhibiting TopoI DNA relaxation activity; others interfere with important enzymes such as thioredoxin, reductase and topoisomerase,<sup>86</sup> leading to DNA damage. When it comes to DNA damage, also known as genotoxicity, caused by Ag<sup>+</sup> has been verified by numerous works. AshaRani et al.<sup>87</sup> systematically investigated the cellular effects of silver nanoparticles (AgNPs), including cytotoxicity, oxidative stress, and DNA damage. They found that AgNPs induce mitochondrial dysfunction and G2/M cell cycle arrest, primarily through ROS accumulation caused by Ag<sup>+</sup>-mediated disruption of the respiratory chain. DNA damage was dose-dependent and may result from direct interactions of Ag<sup>+</sup> with nucleic acids, leading to structural deformation, functional loss, and reduced intracellular ATP levels.

A similar investigation was carried out by Swanner et al.,<sup>88</sup> who treated triple-negative breast cancer (TNBC) cells with PVP-coated AgNPs and observed a significant increase in bulky DNA adducts (Figure 5B). They hypothesized that this was primarily driven by Ag<sup>+</sup>-induced ROS generation, a mechanism supported by the reduction in cytotoxicity upon antioxidant treatment.<sup>89, 90</sup> Further studies revealed that intracellular degradation of AgNPs released Ag<sup>+</sup> ions, which not only promoted oxidative DNA damage but also disrupted redox homeostasis and triggered endoplasmic reticulum stress. This led to S-phase cell cycle arrest and apoptosis in TNBC cells, while sparing non-malignant breast epithelial cells. The released Ag<sup>+</sup> acted as an active disruptor of genomic integrity; their interaction with DNA resulted in conformational changes and impaired repair processes, amplifying cytotoxic effects. The marked upregulation of DNA damage markers such as 53BP1 further confirmed the direct genotoxic role of Ag<sup>+</sup>. This study demonstrates how ions released from NPs can selectively exploit the weaknesses of cancer cells, providing a promising direction for the development of ion-based targeted therapies. In addition to this, there has been a lot of research work on gold and copper complexes as anti-cancer drugs.<sup>91</sup> Most of these complexes follow the principle of binding to important enzymes or proteins in the cell, causing the blockage of specific cellular physiological processes and thus killing the cell. This is still somewhat different from the mechanism of action of Pt, but

each pathway has its significance to try, and these options hold great promise. It is undeniable, however, that there are over 1,000 metal complex drugs in clinical research, only 30 or so Pt drugs are approved for patient use, so for the time being, the Pt and its derivatives have an irreplaceable place in oncology treatment.

### 3. Ion-based therapies

In addition to directly disrupting ionic homeostasis (Section 2), ions can also participate in catalytic or metabolic processes that amplify tumour-killing effects. These ion-assisted strategies often function in combination with other therapeutic modalities. Importantly, such combination approaches are typically driven by clear mechanistic complementarity. For instance, ion-mediated processes can enhance ROS generation, perturb redox balance (e.g., GSH depletion), or sensitise tumour cells to external stimuli such as heat, light, or ultrasound, thereby amplifying therapeutic responses. Recent studies demonstrate their roles in driving Fenton or Fenton-like reactions, disrupting tumour metabolism, and enabling synergistic, multi-modal therapies. Through smart nanoplatforms, ion dynamics can be precisely controlled to enhance oxidative stress, interfere with survival pathways, and improve treatment selectivity.

#### 3.1. Ion-initiated chemo-dynamic therapies

The French chemist Fenton, who originally discovered the Fenton reaction, could not have imagined that today, more than 100 years later, people are actively using such an important chemical reaction to defeat tumours. Interestingly, the Fenton reaction appears particularly suited for tumour therapy because the solid tumour microenvironment is characterised by high acidity, elevated GSH levels, hypoxia, excess H<sub>2</sub>O<sub>2</sub>, and physical anti-drug barriers associated with tumour mass formation. Although these features generally represent obstacles to conventional therapies, they can be strategically exploited in Fenton-based and ion interference approaches to induce selective oxidative damage in tumour cells.<sup>92</sup> However, the two key reactions of the Fenton reaction: Fe<sup>2+</sup> + H<sub>2</sub>O<sub>2</sub> = Fe<sup>3+</sup> + OH<sup>·</sup> + HO<sup>·</sup> and Fe<sup>3+</sup> + H<sub>2</sub>O<sub>2</sub> = Fe<sup>2+</sup> + HOO<sup>·</sup> + H<sup>+</sup> take advantage of the excess H<sub>2</sub>O<sub>2</sub> in the tumour to produce ·OH with a strong oxidative killing effect, while alleviating the lack of oxygen situation in the tumour microenvironment.<sup>93</sup> The Fenton reaction has therefore been explored as the focus of research in CDT. Iron ions, Fe<sup>2+</sup> and Fe<sup>3+</sup>, play a key role in these reactions, and therefore, this is a practical application of iron ion interference therapy. Although iron ions are commonly described as catalysts in the Fenton reaction, this is not strictly accurate, since the redox cycling between Fe<sup>2+</sup> and Fe<sup>3+</sup> is not fully symmetrical during the process. It is these natural advantages of the Fenton reaction that have compelled researchers to extensively investigate the use of the Fenton reaction in the treatment of tumours over the past decades, leading to the development of an increasing number of NPs and nanoplatforms, mostly using environmentally responsive strategies that take advantage of the acidic, reducing and



enzymatically responsive nature of the NPs developed to implement tumour therapies that include the generation of strong oxidative radicals or the delivery of toxic drugs.

### 3.1.1. Fe-induced Fenton Reaction

Early tumour Fenton therapy mainly relied on iron oxide nanoparticles, including  $\text{Fe}_3\text{O}_4$  and  $\alpha\text{-Fe}_2\text{O}_3$ , which generate reactive oxygen species such as  $\cdot\text{OH}$  under the acidic conditions of tumour cells. The intrinsic biocatalytic properties of magnetic  $\text{Fe}_3\text{O}_4$  NPs were first reported by Gao et al.<sup>94</sup> Experiments showed that  $\text{Fe}_3\text{O}_4$  could mimic the peroxidase to oxidize organic substrates. And the activity of this catalytic reaction is dependent on  $\text{H}_2\text{O}_2$ , pH, and temperature. However, the limited  $\cdot\text{OH}$  production capacity of iron oxide NPs alone greatly hampers their therapeutic efficacy, so multiple modes of Fenton reaction triggered by iron ions have been developed. For example, Li et al.<sup>95</sup> addressed the insufficient ROS level in tumour cells by loading  $\text{H}_2\text{O}_2$  into polymersomes to construct  $\text{H}_2\text{O}_2/\text{Fe}_3\text{O}_4$ -poly (lactic-co-glycolic acid) (PLGA) NPs (Figure 6A), which serve as an internal oxygen and ROS source. In this system,  $\text{Fe}_3\text{O}_4$  functions as the Fenton catalyst, as confirmed by the  $\cdot\text{OH}$  generation shown in Figure 6B. The more common strategy is to adopt a co-delivery model with spectroscopic chemotherapeutic agents in combination with other blockers, including catalytic enzymes,<sup>96, 97</sup> or to adopt a combination strategy with chemotherapy and other therapies, such as PTT, PDT, and SDT.<sup>98</sup> In addition, the development of novel iron ion precursors is also actively being pursued. In Figure 6C, Liang et al.<sup>99</sup> reported that a porous yolk shell nanostructure of  $\text{Fe}/\text{Fe}_3\text{O}_4$

(PYSNPs), promoting Zero-valent ( $\text{Fe}^0$ )-catalysed Fenton chemistry in the tumour microenvironment for cancer therapy. The PYSNPs were effective in inhibiting the growth of HepG2 cells with an  $\text{IC}_{50}$  of approximately  $20 \mu\text{g}/\text{mL}$ . A different strategy was demonstrated in Figure 6D by Ding et al.<sup>100</sup> who developed a nanoplatfrom mesoporous polydopamine (MPDA) using hydroxy iron oxide ( $\text{FeOOH}$ ) as an iron reservoir to continuously stimulate the production of  $\cdot\text{OH}$  from  $\text{H}_2\text{O}_2$  in tumour cells to achieve a sustained tumour killing effect in the condition of weakly acidic, low  $\text{H}_2\text{O}_2$  homeostasis. The  $\text{Fe}^{2+}$  and  $\text{Fe}^{3+}$  from this NP are constantly interchanged within the cell and therefore sustainably catalyse the Fenton reaction. The results suggest that all these strategies overcome, to some extent, the difficulties of tumour treatment due to the weakly acidic and low  $\text{H}_2\text{O}_2$  homeostasis conditions in the tumour microenvironment.

### 3.1.2. Cu, Zn, and Mn induced Fenton-like reaction

In anticipation of the widespread use of Fenton reactions in tumour therapy, researchers have also rationally designed nanoplatforms based on ions other than iron ions (e.g.  $\text{Cu}^{2+}$ ,  $\text{Mn}^{2+}$ ,  $\text{Ti}^{3+}$ ,  $\text{Co}^{2+}$ ) that can generate strong oxidative radicals, which we refer to as Fenton-like intracellular redox reactions. These reactions are very similar to those mediated by Fe-based NPs in cells, mainly by triggering  $\text{H}_2\text{O}_2$  to generate lethal ROS; and the creation of a  $\text{ZnO}_2$ -based nanoplatform by Chen's group<sup>51</sup> (Figure 7A) and Zhang's group<sup>101</sup> (Figure 7B), where  $\text{Zn}^{2+}$  inhibits the electron transport chain (ETC), triggers an enhanced oxidative stress response, with a rapid rise in ROS causing

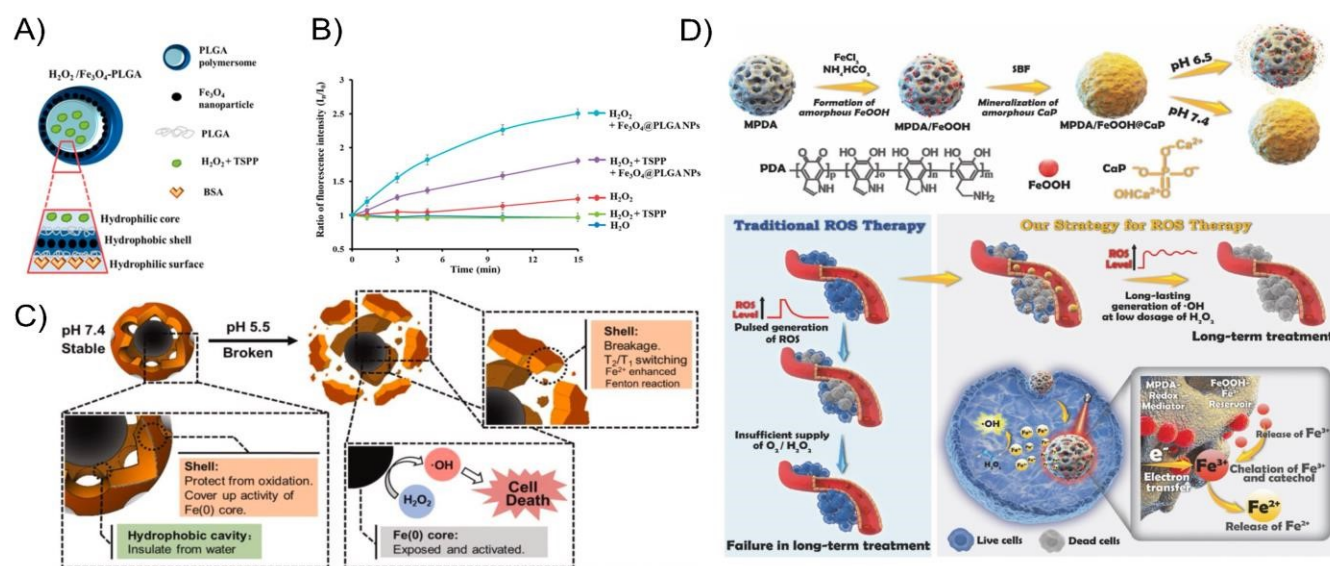


**Figure 6** Fe-based Fenton reaction systems for enhanced ROS generation and therapeutic intervention. (A) Schematic representation of  $\text{H}_2\text{O}_2$ -loaded,  $\text{Fe}_3\text{O}_4$ -embedded poly (lactic-co-glycolic acid) (PLGA) polymersomes ( $\text{H}_2\text{O}_2/\text{Fe}_3\text{O}_4$ -PLGA), fabricated via a double emulsion method. These nanostructures were designed to co-deliver Fe and  $\text{H}_2\text{O}_2$  for local Fenton reaction activation. (B) Time-dependent fluorescence intensity corresponding to  $\cdot\text{OH}$  generation during Fenton reactions under various conditions, including  $\text{H}_2\text{O}$ ,  $\text{H}_2\text{O}_2$  alone, and combinations of  $\text{Fe}_3\text{O}_4@PLGA$  NPs with  $\text{H}_2\text{O}_2$  in the presence or absence of a tetrasodium pyrophosphate (TSPP) stabilizer. Enhanced  $\cdot\text{OH}$  production was observed in  $\text{Fe}_3\text{O}_4/\text{H}_2\text{O}_2$  systems, indicating effective catalytic activity. (A, B) Reproduced with permission.<sup>95</sup> Copyright 2016, American Chemical Society. (C) Schematic illustration of the pH-responsive Fe release behaviour of porous yolk shell nanostructure of  $\text{Fe}/\text{Fe}_3\text{O}_4$  (PYSNPs) and the resulting intracellular ROS burst, highlighting the acidic tumour microenvironment as a trigger for catalytic Fenton reaction. Reproduced with permission.<sup>99</sup> Copyright 2020, Elsevier. (D) Diagram depicting the synthesis of  $\text{MPDA}/\text{FeOOH}@CaP$  NPs through  $\text{FeOOH}$  precipitation and  $\text{CaP}$  biomineralization. The particles exhibit long-lasting Fenton-like catalytic activity in the tumour environment, enabling sustained ROS production and therapeutic efficacy through a synergistic catalytic-therapeutic mechanism. Reproduced with permission.<sup>100</sup> Copyright 2021, Wiley-VCH GmbH.



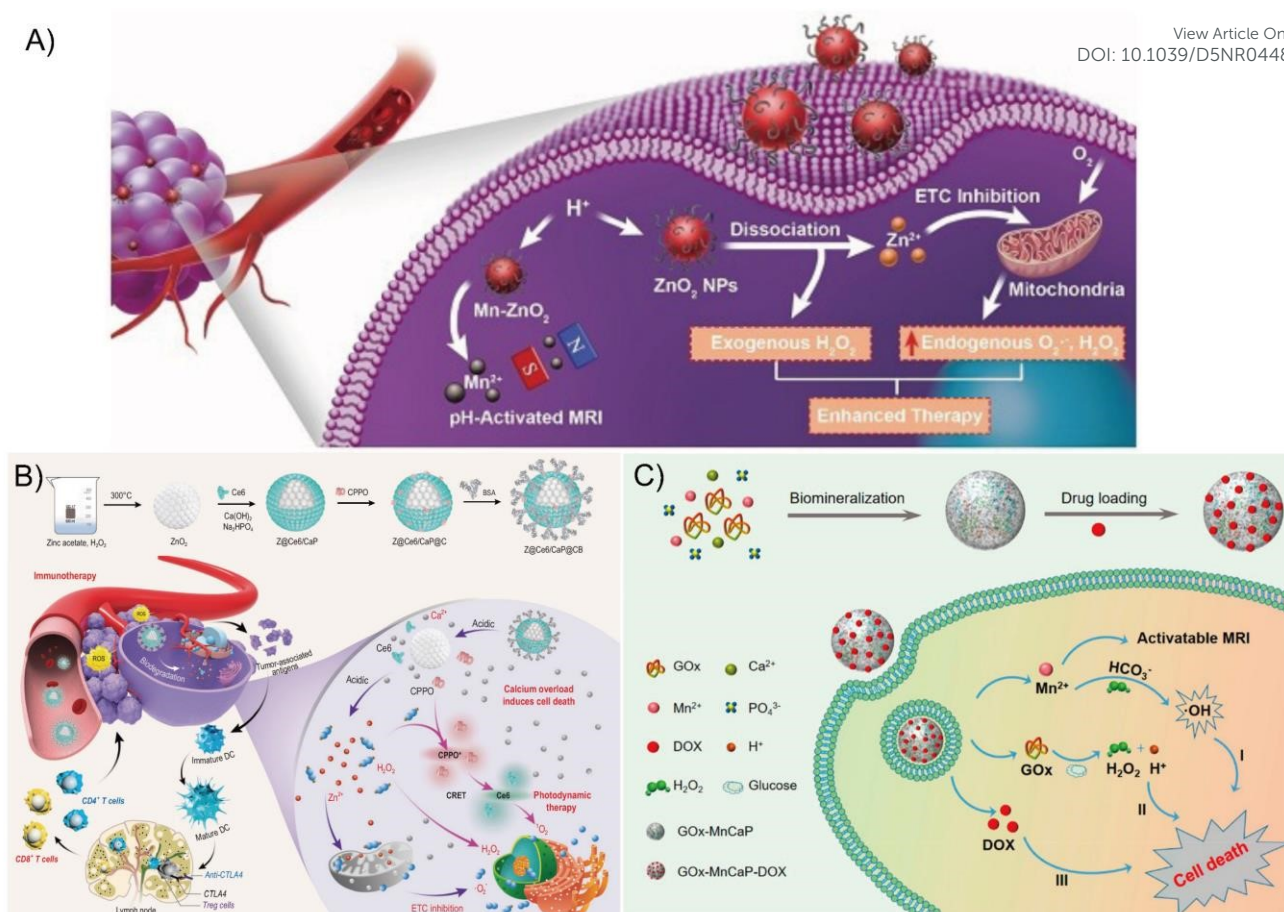


**Figure 7** Cu, Zn, and Mn-driven Fenton-like catalytic platforms for enhanced reactive oxygen species (ROS)-mediated cancer therapy. (A) Schematic illustration of multifunctional Mn-doped ZnO<sub>2</sub> NPs (ZnO<sub>2</sub> NPs) for magnetic resonance imaging (MRI)-guided and oxidative stress-amplified cancer treatment. After endocytosis by tumour cells, ZnO<sub>2</sub> NPs decompose under mildly acidic conditions, releasing Zn<sup>2+</sup> and H<sub>2</sub>O<sub>2</sub>. The released Zn<sup>2+</sup> disrupts the electron transport chain, enhancing mitochondrial O<sub>2</sub><sup>-•</sup> and H<sub>2</sub>O<sub>2</sub> generation. Meanwhile, Mn<sup>2+</sup> incorporation provides pH-activated T<sub>1</sub>-weighted MRI contrast capability. Reproduced under the terms of the CC-BY license.<sup>51</sup> Copyright 2019, Lin et al. (B) Illustration of the synthesis and cascade therapeutic mechanism of Z@Ce6/CaP@CB nanobombs. Zinc peroxide nanospheres (ZnO<sub>2</sub>) were coated with a CaP shell encapsulating chlorin e6 (Ce6) via an in-situ template-assisted method (Z@Ce6/CaP), followed by surface modification with bis[2,4,5-trichloro-6-(pentylloxycarbonyl)phenyl] oxalate (CPPO) and bovine serum albumin (BSA) to obtain Z@Ce6/CaP@CB. These NPs induce intracellular Ca<sup>2+</sup> overload and sequential ROS bursts (H<sub>2</sub>O<sub>2</sub>, <sup>1</sup>O<sub>2</sub>, and O<sub>2</sub><sup>-•</sup>), triggering cell apoptosis and systemic immune activation. The cascade proceeds without external stimulation, offering potent inhibition of both primary and distant tumour progression. Reproduced under the terms of the CC-BY license.<sup>101</sup> Copyright 2021, Yang et al. (C) Schematic representation of the synthesis and therapeutic mechanism of GOx-MnCaP-DOX NPs. The system integrates Mn<sup>2+</sup>-mediated Fenton-like chemodynamic therapy (I), glucose oxidase (GOx)-induced starvation therapy (II), and doxorubicin (DOX)-based chemotherapy (III), enabling multimodal and MRI-monitored antitumor effects. Reproduced with permission.<sup>105</sup> Copyright 2019, American Chemical Society.

significant damage to tumour cells. In the work of Chen's group, ZnO<sub>2</sub> was used as the primary antitumour agent, while in the work of Zhang's group, ZnO<sub>2</sub> was used in combination with CaP, where Zn<sup>2+</sup> stimulated H<sub>2</sub>O<sub>2</sub> to produce superoxide anions (O<sub>2</sub><sup>-•</sup>) in addition to stimulating co-encapsulating bis[2,4,5-trichloro-6-(pentylloxycarbonyl)phenyl] oxalate (CPPO)-mediated chemiexcited photodynamic therapy, as well as Ca<sup>2+</sup> to enable calcium overload therapy. It is worth mentioning that in addition to its catalytic function, similar to that of iron ions, extensive experiments have shown that Zn is also involved in protein structure, transcriptional regulation, and zinc signalling, and Zn-based tumour therapies developed based on these physiological processes are emerging.<sup>102, 103</sup> This suggests that the dynamic balance of Zn ions is also a target with great potential for development. Another ion (Mn<sup>2+</sup>) has good biocompatibility and high spin number and therefore can also mimic the Fentonian response of Fe and Zn ions in the tumour

environment. Some work has indeed utilized Mn<sup>2+</sup> to catalyse the production of -OH from H<sub>2</sub>O<sub>2</sub> in vivo as a Fenton-like reaction or CDT.<sup>104</sup> Fu et al. achieved cascade cooperative cancer treatment using Mn<sup>2+</sup> and glucose oxidase (Gox), via Mn<sup>2+</sup>-mediated Fenton response and GOx-mediated starvation therapy, shown in the Figure 7C.<sup>105</sup> Moreover, the high valence state of manganese itself acts as a storage pool for H<sub>2</sub>O<sub>2</sub>, providing an abundant ROS source for CDT, solving the problem of inefficiency due to the shortage of reactants for CDT. In summary, the various cases above are all tumour-killing mechanisms based on ion-triggered Fenton or Fenton-like reactions, but these strategies are not completely disconnected from each other, meaning that homeostatic regulation may also be involved in triggering CDT, regulating intracellular ion homeostasis while also blocking certain intracellular signalling. Taken together, these therapeutic tools can only be additively effective.



### 3.2. Ions as biocatalysts for fuel and H<sup>+</sup> /GSH consumption

Interestingly, some ions can act as scavengers in addition to initiating chemical reactions in the cell, such as the Fenton reaction. These ionic bullets with specific properties can use GSH, H<sup>+</sup>, and tumour nutrients as targets. On the one hand, the removal of the strongly reducing GSH from tumour cells can lead to an inability to scavenge oxidative free radicals and increase their killing capacity, which is a beneficial adjunct to CDT. On the other hand, the removal of H<sup>+</sup> has a very important role in alleviating the acidic tumour microenvironment, as the reduction of H<sup>+</sup> can cause the tumour microenvironment to deviate from its original state; in other words, we can also view such strategies of depleting GSH and H<sup>+</sup> as a disruption of the homeostatic balance of the tumour. Needless to say, reduced GSH in tumour cells can be used well for triggering, thus minimizing damage to normal cells. However, on further reflection, there must be a reason why GSH is present in greater amounts in tumour cells than in normal cells. Therefore, disruption of the GSH balance in tumour cells, i.e., GSH deprivation, can affect cellular physiological processes. Many efforts have been made to develop compounds of Mn, Fe, Cu, and Pt ions that can be used to oxidize and deplete GSH.<sup>106</sup> It is important to note that GSH triggering and GSH deprivation strategies are to some extent interlinked, and in most cases, the process of GSH triggering nanosystems is also a depletion process. Obviously, this is a similar strategy to the one presented in section 2.1, whereas 2.1 focused on smaller chemical-physical processes within the cell, the one presented here focuses on a larger picture, such as the tumour clump/tissue. This modulation of the tumour microenvironment using ions can essentially affect the sensitivity of the tumour to drugs or other therapeutics, because a tumour cell's steady state is disturbed (as it struggles to restore its homeostatic balance). This approach gives a combinatorial treatment strategy. In addition, the maintenance of the physiological activity of tumour cells also depends on the metabolism of nutrients to produce energy, so seeking to block the source of nutrients to tumour cells is also a reliable strategy. Current efforts to block tumour energy supply based on influencing metabolic pathways include depleting the substrates glucose and glutamine or blocking the mitochondrial energy metabolic chain. All of these tumour treatment strategies are based on the biocatalytic capacity of ions; in other words, we can think of these ions with some catalytic capacity as biocatalysts.

In fact, the glucose removal tumour starvation treatment strategy has achieved better efficacy. Various groups, including Han,<sup>107</sup> Huang<sup>108</sup> and Xiang et al.,<sup>109</sup> have used GOx to convert one of the energy sources of tumour cells, glucose, to metabolic waste in order to cut off their energy source; Shi's group used 2-deoxy-D-glucose (2DG) as an antiglycolytic agent to restrict the glucose metabolism of tumour cells to achieve a similar effect in tumour therapy (Figure 8A).<sup>110</sup> In Shi's work, a glycolysis inhibitor was combined with black phosphorus (BP) nanosheets to achieve synergistic metabolic suppression. The

two-dimensional morphology of BP nanosheets facilitates intimate membrane interaction and efficient intracellular internalisation, while their large reactive surface area accelerates degradation under physiological conditions. Upon degradation within tumour cells, BP nanosheets release PO<sub>4</sub><sup>3-</sup> species that accumulate in lysosomes and consume protons, forming HPO<sub>4</sub><sup>2-</sup> and thereby perturbing intracellular pH homeostasis. The nanosheet structure is critical for maximising interfacial reactivity and degradation kinetics, which in turn amplifies the ion-mediated energetic deprivation effect. However, it can actually be seen that a number of ions that can be used to detect glucose have been developed as glucose detection reagents.<sup>111</sup>

On the other hand, these complexes show good glucose binding ability, so the development of drugs based on these ions with the ability to detect and deplete at the same time is just around the corner, and undoubtedly, the associated toxicological and pharmacological experiments will have to be carried out. The energy source for tumour metabolism is not only glucose but also relies on glutamine; however, to date, tumour therapies targeting glutamine depletion or targeting glutamine have not been fully developed and explored, but the prospects for therapeutic approaches to truncate glutamine should not be overlooked.<sup>112, 113</sup> Some small molecules, such as 6-diazo-5-oxo-L-norleucine (DON),<sup>114</sup> have been used to explore glutamine blocking therapies with promising results, and we believe that truncation therapies using ion interference with glutamine will be developed soon. A great deal of work has also focused on the use of high GSH in the tumour microenvironment as a trigger switch, triggering a number of subsequent responses. At the same time, GSH can also be depleted, which is also a form of depletion therapy. The use of ion interference to achieve depletion of intracellular nutrients continues to be investigated. Zhang et al.<sup>115</sup> have designed a polyvinyl pyrrolidone (PVP)-modified magnesium silicide (Mg<sub>2</sub>Si, MS) NP, shown as Figure 8B, that deprive tumours of oxygen (essential for tumour growth and angiogenesis) within the tumour, thereby effectively implementing tumour starvation therapy. The Mg<sub>2</sub>Si NPs remove oxygen from the tumour and generates SiO<sub>2</sub> aggregates to block capillary generation, forming a sealed, self-consuming system. The results show that even at a very low dosage of Mg<sub>2</sub>Si NPs (2 mM), the proliferation of cells can be inhibited by up to 50% within 24h, and this only occurs when very low levels of cellular hypoxia are induced. Liu's group adopted the strategy of oxygen and glucose dual deprivation and achieved a good growth inhibition effect on 4T1 cells (Figure 8C).<sup>116</sup> The team used banoxantrone dihydrochloride (AQ4N) to activate tumour hypoxia, while GOx was used to further block glucose assimilation and thus oxygen deprivation, achieving a synergistic and enhanced anti-tumour effect. In addition to oxygen, the proton (H<sup>+</sup>) has been identified as a crucial component of the tumour microenvironment, serving as a viable target to develop therapeutic interventions. Some work has used H<sup>+</sup> depletion to alleviate the acidity of the tumour microenvironment, indirectly altering the stable environment for tumour growth, resulting in a decrease in tumour cell viability or drug tolerance, and achieving good tumour



therapeutic effects. Almost the same strategy was used by Yu's team,<sup>117</sup> with the difference that the group went further by combining GSH elimination to achieve a cross-linking of the three modalities. Overall, ion-based strategies for depriving tumours of various key substances are of great research interest.

### 3.3. Synergistic therapy

Synergistic therapy is where two or more therapies complement and enhance each other to overcome the unfavourable microenvironment within the tumour tissue. This strategy is now widely adopted and generally involves a combination of two therapies or multimodal therapies. As mentioned earlier, many therapies involving ions are CDT involving the Fenton reaction; generally, one adopts a strategy in combination with PDT, acoustodynamic therapy, or emerging immunotherapy.

#### 3.3.1. Two-modal combined therapy

The ions produced by the transition metal oxides (especially in the highly oxidized state, e.g.,  $Mn^{4+}$ ,  $Cu^{2+}$ ) have a strong catalytic capacity for the Fenton reaction, which reduces  $H_2O_2$  to produce ROS through the gain or loss of their own electrons. Molybdenum-based ( $Mo^{5+/6+}$ ) NPs have an interesting intracellular interconversion between the two valence states, allowing CDT and PDT to be synergized. As illustrated in Figure 9A, Liu et al.<sup>118</sup> reported a  $Mo_2C$ -derived polyoxometalate (POM) CDT agent in which  $Mo^{5+}$  was oxidized to  $Mo^{6+}$  by  $H_2O_2$  and accompanied by a large amount of singlet oxygen ( $^1O_2$ ) production;  $Mo^{6+}$  is reduced by GSH to  $Mo^{5+}$  in an environment with sufficient GSH in tumour cells, achieving a "green chemistry"-like outcome. What is more interesting is that  $Mo^{5+}$  will produce PTT under near-infrared (NIR) irradiation, thus enabling a combined PTT/CDT therapy. The common Fe(II) can also shine in a different light when combined with two-dimensional (2D) nanomaterials. Many 2D nanomaterials have good photothermal conversion capabilities according to current

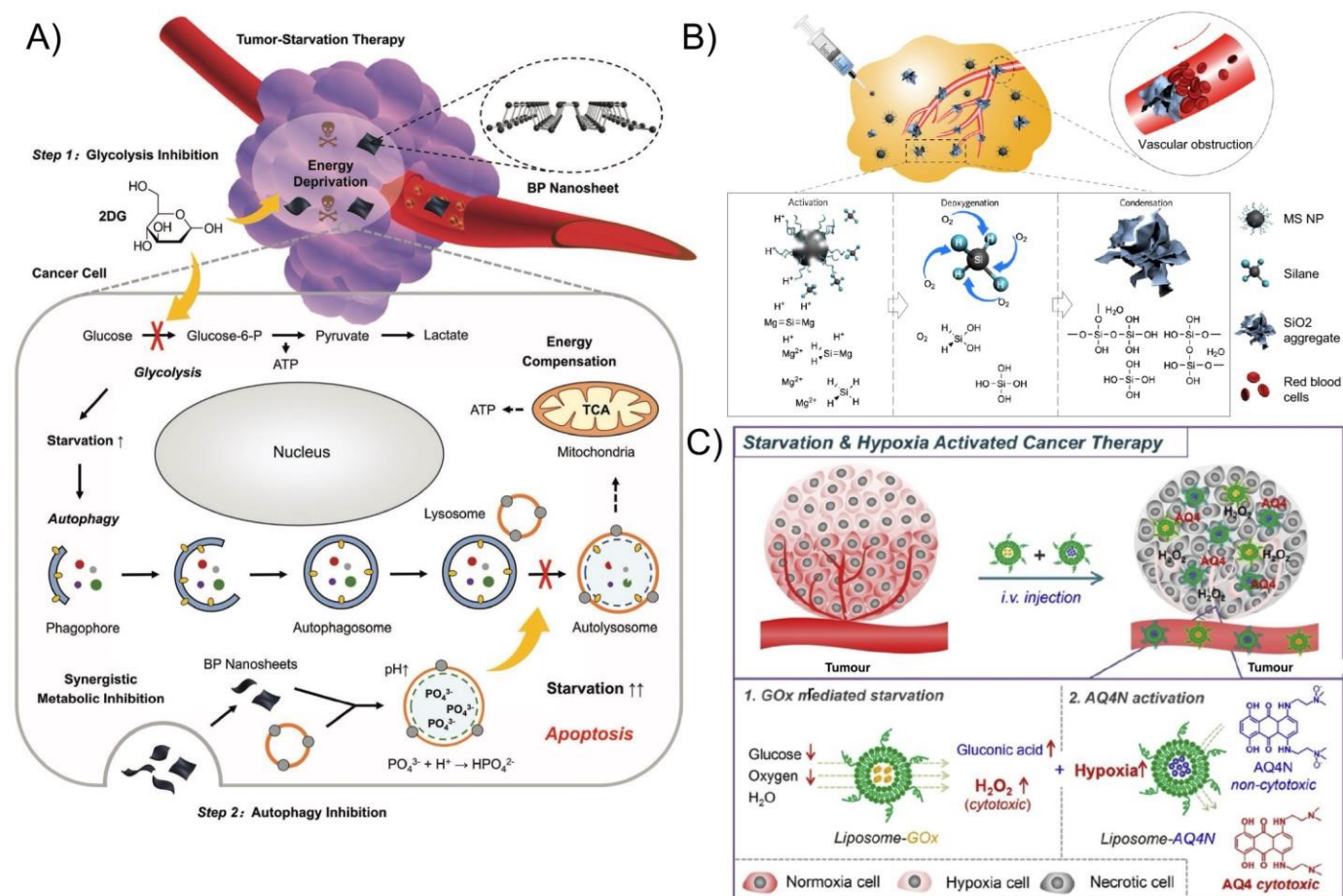


**Figure 8** Representative strategies leveraging ions or ionic materials as biocatalysts to promote fuel consumption or interfere with cellular reductive environments ( $H^+$ /GSH) to induce metabolic disruption or starvation in tumours. (A) Schematic illustration of autophagy inhibition-augmented starvation therapy. Cancer cell glycolysis is blocked by 2-deoxy-d-glucose (2DG), inducing energy deprivation, while black phosphorus (BP) nanosheets inhibit protective autophagy, cutting off the compensatory nutrient supply and ultimately triggering apoptosis. Reproduced under the terms of the CC-BY license.<sup>110</sup> Copyright 2020, Bowen Yang et al. (B) Schematic representation of acidic tumour microenvironment-responsive  $Mg_2Si$  nanoparticles (MS NPs), which produce reactive silanes for in situ oxygen consumption and generation of silica ( $SiO_2$ ) clots in tumour vasculature, thereby preventing reoxygenation and sustaining deep tumour hypoxia. Reproduced with permission.<sup>115</sup> Copyright 2017, Springer Nature. (C) Design of a liposome-based co-delivery platform integrating glucose oxidase (GOx) and hypoxia-activated prodrug banoxantrone dihydrochloride (AQ4N). This nanoplatform synergistically induces starvation and enhances the therapeutic efficacy under hypoxic conditions by consuming glucose and oxygen within tumours. Reproduced with permission.<sup>116</sup> Copyright 2018, Elsevier.



research, which provides excellent opportunities for PTT.<sup>119</sup> Titanium carbide (Ti<sub>3</sub>C<sub>2</sub>) used by Wu et al.<sup>120</sup> has an extinction coefficient of 24.82 L/g·cm when loaded with Fe, which is superior to Au nanocluster and graphene oxide, and can reach 45 degrees after 600 s of irradiation with 808 nm light (1.5 W/cm<sup>2</sup>); moreover, the loaded Fe<sup>2+</sup> can catalyse the Fenton reaction, constituting a two-mode synergistic nanoplatform. A large number of combined 2-modality cancer therapies are suggested in this review.<sup>121</sup>

Immunotherapy is currently of considerable interest, and ion-involved enhanced immunotherapy has been developed in succession. Some have adopted the strategy of using ions to induce immunogenic death, with Sun et al.<sup>122</sup> using loaded Mn<sup>2+</sup> (Figure 9C) to catalyse the production of free radicals from H<sub>2</sub>O<sub>2</sub>, thereby inducing tumour-associated antigen presentation and recruiting T cells to enrich at the tumour site. Others have targeted tumour-associated macrophages (TAMs). For example, Gu et al.<sup>123</sup> used iron ions to regulate the mitochondrial metabolism of TAMs, thereby causing a paradigm shift in intracellular free radical metabolism from oxidative phosphorylation to glycolysis, and demonstrated that iron ion-induced ferroptosis stress can drive TAMs to mount a powerful attack on tumour cells (Figure 9D).

### 3.3.2. Multi-modal therapy

Further additions of response modes to a nanosystem are emerging, which form the so-called “all-in-one” model. Wang et al.<sup>124</sup> adopted a strategy of PDT in combination with CDT and then SDT (Figure 9B). The synthesized Janus nanocomplex upconversion NPs (UCNPs), denoted as UPFBs, can be driven by ultrasound and 808 nm NIR to produce SDT and PDT, while CDT is induced by iron ion-containing ferrous zirconium porphyrin metal organic framework [PCN-224(Fe)]. Specifically, they have constructed UPFBs a core@shell@shell architecture comprising NaYF<sub>4</sub>: 20%Yb, 1%Tm@NaYF<sub>4</sub>: 10%Yb@NaNdF<sub>4</sub> and MOFs [PCN-224(Fe)]. UCNPs can convert NIR light into Ultraviolet-visible light to stimulate MOFs [PCN-224(Fe)] to produce PDT, while Fe<sup>2+</sup> in MOFs [PCN-224(Fe)] catalyses the Fenton reaction to generate ROS, and this process can be enhanced by ultrasound stimulation of SDT. The results show that in vitro cell viability decreases to 16.7% under the combined PDT/SDT/CDT treatment; tumours are also eliminated in mice, and no systemic toxicity is observed. In fact, combining multiple therapies is challenging. It requires not only a clear understanding of the strengths and weaknesses of the various therapies but also the creation of appropriate systems to ensure that the individual therapies are mutually reinforcing, and this will require further research.

## 4. Ions for imaging-guided therapy

Imaging-guided ion-based therapies have attracted increasing attention due to their potential to improve treatment precision and enable real-time monitoring. In these systems, imaging components are often integrated with ion-mediated therapeutic processes, allowing visualisation of treatment localisation, ion release behaviour, or downstream biological responses. Importantly, in most cases, ion interference remains



**Figure 9** Representative nanoplatforms for synergistic cancer therapies integrating photothermal therapy (PTT), chemodynamic therapy (CDT), sonodynamic therapy (SDT), immunotherapy, ferroptosis, and photodynamic therapy (PDT). (A) Schematic illustration of the synthesis and mechanism of Mo<sub>2</sub>C-derived polyoxometalate (POM) nanoclusters as a dual-functional PTT/CDT agent. Under mildly acidic tumour conditions, POM self-assembles, enhancing NIR-II absorption (1060 nm) and enabling deep tissue photothermal conversion. Oxidation of Mo<sup>5+</sup> to Mo<sup>6+</sup> generates cytotoxic singlet oxygen (<sup>1</sup>O<sub>2</sub>) via the Russell mechanism, while CDT is enhanced through photothermal effects and GSH depletion. NIR-II photoacoustic imaging guides precise therapy, achieving effective tumour ablation and preventing recurrence. Reproduced with permission.<sup>118</sup> Copyright 2019, Wiley-VCH GmbH. (B) Schematic illustration of the multifunctional Janus nanocomplex nanoplatform (denoted as UPFB) for synergistic cancer therapy. The Janus-structured NPs, composed of upconversion nanoparticles (UCNPs) and porphyrin-based MOFs (PCN-224(Fe)), are surface-modified with biotin for tumour targeting. Upon NIR (808 nm) laser irradiation, the UCNPs activate the MOFs to initiate Type II PDT, while catalase-like activity of PCN-224(Fe) decomposes endogenous H<sub>2</sub>O<sub>2</sub> to O<sub>2</sub>, relieving tumour hypoxia. The system also enables SDT under ultrasound (US) and multimodal imaging, including fluorescence and T<sub>2</sub>-weighted MRI. GSH depletion further amplifies ROS generation, collectively promoting apoptosis and potent antitumor effects. Reproduced with permission.<sup>124</sup> Copyright 2021, American Chemical Society. (C) Schematic diagram of PEGylated Au@HMnMSNs (hollow mesoporous silica-coated, Mn-doped gold nanoparticles) loaded with doxorubicin (DOX) and Aspirin (ASA), functioning as immunogenic cell death (ICD) nanoinducers. These cascade nanoinducers consume GSH to release Mn<sup>2+</sup> for Fenton-like ·OH generation. The gold core exhibits GOx-mimetic activity, converting glucose into gluconic acid and H<sub>2</sub>O<sub>2</sub>, which is then further used to generate O<sub>2</sub>, enhancing catalytic activity. This multi-step cascade promotes dendritic cell maturation and synergizes with immunotherapy. Reproduced with permission.<sup>122</sup> Copyright 2021, Wiley-VCH GmbH. (D) Schematic representation of MIL88B/RSL3-mediated metabolic reprogramming of tumour-associated macrophages. The MIL88B (iron MOF) and ferroptosis inducer RSL3 synergistically induce lipid peroxidation and mitochondrial disruption, shifting macrophage metabolism from oxidative phosphorylation to glycolysis. This transition counteracts M2 polarization signals and activates M1-associated transcription factors, leading to potent tumoricidal effects including phagocytosis and metastasis suppression. Reproduced with permission.<sup>123</sup> Copyright 2021, American Chemical Society.

the primary therapeutic mechanism, while imaging serves as a complementary tool for guidance and evaluation. For example, nanoplatforms designed for Fenton or ion-release-based therapies can incorporate imaging functionalities to monitor tumour accumulation and therapeutic progression. In some systems, imaging primarily provides auxiliary support, whereas the ion-mediated processes drive the therapeutic outcome. Overall, the integration of imaging and ion interference offers a



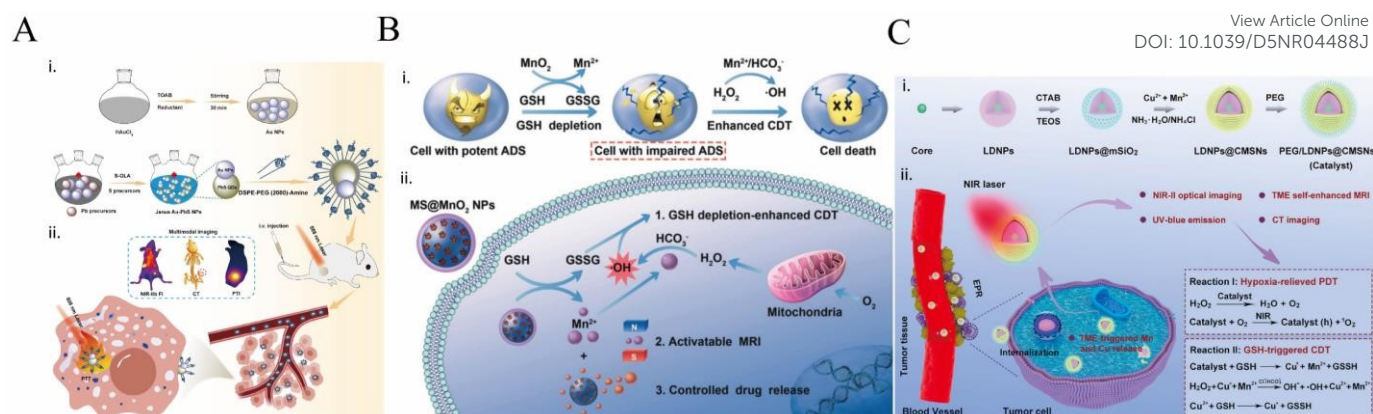


**Figure 10** Schematic representations of ion-based nanoplatforms for imaging-guided cancer therapy. (A) Schematic illustration of the synthesis and application of Janus Au–PbS NPs for multimodal imaging-guided PTT. i) Au NPs are first synthesized and combined with Pb and sulfur precursors to form Janus Au–PbS NPs. These are subsequently modified with 1,2-distearoyl-sn-glycero-3-phosphoethanolamine-N-[amino(polyethylene glycol)-2000] (DSPE-PEG<sub>2000</sub>-Amine) for improved biocompatibility. ii) The NPs aggregate in tumours after intravenous injection, allowing for precise photothermal ablation of tumour cells initiated by an 808 nm laser, as well as NIR-IIb fluorescence imaging (FI), CT, and photothermal imaging (PTI). Reproduced with permission.<sup>126</sup> Copyright 2024, American Chemical Society. (B) Schematic illustration of MS@MnO<sub>2</sub> nanoparticles as multifunctional agents for MRI-guided CDT. i) MnO<sub>2</sub> nanoparticles are reduced by intracellular GSH, leading to GSH depletion and the generation of Mn<sup>2+</sup> ions. The impairment of the cellular antioxidant defence system (ADS) enhances oxidative stress. Mn<sup>2+</sup> subsequently catalyses a Fenton-like reaction with endogenous H<sub>2</sub>O<sub>2</sub> in the presence of HCO<sub>3</sub><sup>-</sup>, producing highly reactive hydroxyl radicals that induce cell death. ii) The effectiveness of CDT is increased when MS@MnO<sub>2</sub> NPs cause GSH depletion upon endocytosis by tumour cells. The released Mn<sup>2+</sup> also enables T<sub>1</sub>-weighted MRI for real-time diagnosis and treatment monitoring. Additionally, the nanoplatform allows for controlled drug release in response to the tumour microenvironment. Reproduced with permission.<sup>136</sup> Copyright 2018, Wiley-VCH GmbH. (C) Schematic representation of PEG/lanthanide-doped NP (LDNP)@Cu/Mn silicate nanosphere (CMSN) nanoplatforms for tumour microenvironment- and NIR laser-responsive multimodal cancer theranostic. i) Stepwise synthesis involves LDNP core formation, mesoporous silica coating, Cu<sup>2+</sup>/Mn<sup>2+</sup> loading, and PEGylation to enhance biocompatibility. ii) Upon accumulation in tumour tissue via the enhanced permeability and retention (EPR) effect, the nanoparticles are internalized by tumour cells. Within the tumour microenvironment (TME), elevated levels of H<sub>2</sub>O<sub>2</sub> and GSH trigger the release of Cu and Mn ions, initiating two therapeutic pathways: Hypoxia-relieved PDT and GSH-triggered CDT. In addition to synergistic PDT/CDT effects, the system supports NIR-II fluorescence imaging, tumour microenvironment-enhanced MRI, and CT imaging, enabling precise diagnosis and treatment monitoring. Reproduced with permission.<sup>144</sup> Copyright 2020, American Chemical Society.

promising strategy to enhance treatment accuracy without altering the fundamental mechanism of ion-induced tumour suppression.

#### 4.1. Au NP for fluorescence image

While ion intervention or ion modulation-based tumour therapy represents a rapidly expanding field with great potential, ion-assisted imaging technologies have also advanced significantly. Gold-based nanomaterials, for instance, have been widely explored as contrast agents for computed tomography (CT), photoacoustic, and surface-enhanced Raman scattering (SERS) imaging, and can also serve as fluorescent or NIR probes when functionalised with suitable dyes. These ion-assisted visualization methods have provided important assistance in the early diagnosis and real-time monitoring of various diseases, particularly tumours, and have become an important part of modern tumour therapy.

Au NPs are good PPT initiators, and enormous Au nano-PTT initiation platforms from NIR(I) to NIR(III) have been developed.<sup>125</sup> It is because of its ability to produce a temperature different from that of normal tissue when stimulated by light (photothermal conversion effect) that its therapeutic effect at the tumour site can be monitored in real time by means of a temperature measurement instrument. Exploiting this photothermal tunability, Xue-Hui et al.<sup>126</sup> developed plasmonic-fluorescent Janus Au–PbS NPs with dual-modality NIR-IIb fluorescence/CT imaging and PTT capabilities (Figure 10A). Crucially, their mechanistic study revealed that electron transfer from Au to PbS quantum dots in the Janus

architecture stabilizes NIR-IIb fluorescence while preserving the photothermal efficiency of Au, thus overcoming the inherent competition between optical emission and thermal conversion in conventional hybrid systems. This electronic synergy enabled real-time tumour tracking and optimized ablation under multimodal guidance. In addition, Janus magneto-plasmonic nanostructures, such as Au–Fe<sub>3</sub>O<sub>4</sub> systems, have been developed to integrate magnetic guidance with photothermal therapy, enabling enhanced tumour targeting and improved treatment efficiency.<sup>127</sup>

Using Au NPs as a short imaging time, low nephrotoxicity CT contrast agent, Kim et al. demonstrated on prostate cancer LNCaP cells that the cells treated with PEG-coated Au NPs had more than 4-fold higher CT intensity compared to the control group.<sup>128</sup> As the gold surface is more easily modified by thiol groups,<sup>129</sup> some fluorescent groups have also been modified on Au NPs, which has achieved the effect of fluorescent probes.<sup>130, 131</sup> Attributed to the fact that Au NPs are a hyper-efficient quencher, the trajectory of the drug in vivo can be dynamically represented by the lighting and quenching of fluorescent molecules. Zhang's group developed a rhodamine B-conjugated, caspase-responsive peptide–gold NP construct (RB-DEVD–AuNP–DTP) that integrates dual targeting and pro-apoptotic functions. Owing to its surface-engineered fluorescence resonance energy transfer (FRET) property, this nanosystem enables simultaneous induction of apoptosis and real-time visualization of the apoptotic process.<sup>132</sup>

In a related study, a matrix metalloproteinase (MMP)–responsive FRET system combining gold nanoparticles (AuNPs)



and quantum dots (QDs) was developed to monitor tumour microenvironments in real time.<sup>133</sup> Under MMP-rich conditions, AuNPs and QDs were induced to form clusters through enzyme-triggered coupling, bringing the particles into close proximity and resulting in fluorescence quenching of the QDs via FRET. The extent of fluorescence change was found to correlate strongly with MMP activity, tumour burden, and growth stage, enabling non-invasive tracking of tumour progression in vivo. This work exemplifies how the optical and electronic characteristics of gold-based nanostructures can be exploited not only for tumour imaging but also for dynamic feedback on therapeutic responses, reinforcing the role of ion-derived nanomaterials in imaging-guided therapy.

#### 4.2. Ions for MRI

MRI is currently a widely used imaging technique for identifying and localizing tumours. This monitoring treatment of tissue in the body relies significantly on well-formulated contrast agents. Among them, IONPs serve as effective  $T_2$  contrast agents, in addition to their function as “ion bullets” described in Section 3.1.1. Typically 5–12 nm in diameter, these NPs can be further encapsulated in glucan to prolong their in vivo circulation.<sup>133, 134</sup> Moreover,  $Mn^{2+}$  is an effective  $T_1$  MRI contrast agent owing to its five unpaired electrons, which provide strong paramagnetism and short electron relaxation time, resulting in positive signal enhancement.<sup>135</sup> Recent studies have exploited this property by incorporating  $Mn^{2+}$  into multifunctional nanoplatforms that enable simultaneous therapy and MRI monitoring of critical therapeutic parameters such as drug targeting and tumour regression. For instance, Lin et al.<sup>136</sup> demonstrated that  $Mn^{2+}$  can act as both a Fenton-like catalyst and a  $T_1$  MRI contrast agent, achieving synergistic therapeutic and diagnostic benefits (Figure 10B). This integration of diagnostic and therapeutic functions represents a key trend in modern nanomedicine, as the absence of real-time feedback often limits treatment efficacy.

In addition, barium-based nanomaterials (e.g., barium titanate, BT) have been developed as second-harmonic generation (SHG) nanoprobe, offering narrow emission spectra and resistance to signal saturation—advantages not attainable with conventional imaging agents.<sup>137, 138</sup>  $Cu^{2+}$ -assisted positron emission tomography (PET) imaging further enables *in vivo* real-time quantitative tracking of therapeutic processes.<sup>15</sup> Interestingly, when several metal ions are integrated into a single nanocomposite, multiple imaging modalities can be simultaneously achieved by harnessing their individual physicochemical properties.<sup>139–141</sup> Other ions such as  $Gd^{3+}$  complexes<sup>95</sup> and  $Zn^{2+}$ -based probes<sup>142, 143</sup> also enhance MRI signals or contrast ratios, providing valuable tools for precise tumour localization.

#### 4.3. NIR-II fluorescence imaging-guided ion therapy

NIR-II (1000–1700 nm) can provide a deeper-tissue penetration than light in other wavelengths, as well as higher spatial resolution. The use of NIR II probes can reduce the occurrence of photon scattering and autofluorescence. As Figure 10C

clearly shows, Xu et al.<sup>144</sup> synthesized copper/manganese silicate nanosphere (CMSN)-coated lanthanide-doped nanoparticles (LDNPs@CMSNs). The core-shell structure of the LDNPs is doped with four ions,  $Yb^{3+}/Er^{3+}/Tm^{3+}/Ce^{3+}$ , enabling a transition of the excitation pattern from NIR to UV-Blue. This NP loaded with multiple ions showed a significant improvement in light utilization efficiency and anti-tumour effect. The NIR II emission of the NPs was increased by 12.3-fold with  $Ce^{3+}$  doping; in vitro 3-(4,5-dimethylthiazol-2-yl)-2,5-diphenyltetrazolium bromide (MTT) assays showed a decrease in cell viability to 8.6% after NP application and light irradiation, and a significant inhibition of tumour growth in mice. Some ions are preferred as NIR II imaging probes, such as  $Er^{3+}$  and  $Nd^{3+}$ .<sup>145, 146</sup> It has to be said that the current approach to NIR II-assisted tumour therapy is developing rapidly, and this field will also provide new paths for tumour visualization therapies.

#### Conclusions

Ion interference therapy is a promising tumour treatment strategy that acts by perturbing intracellular ionic homeostasis, enhancing Fenton or Fenton-like reactions, regulating intracellular signalling pathways, and in some cases enabling imaging-guided therapy. Although various ions, such as  $Ca^{2+}$ ,  $Na^+$ ,  $Fe^{2+}/Fe^{3+}$ ,  $Cu^{2+}$  and  $Mn^{2+}$ , have been widely explored for tumour therapy, further in-depth investigations are still required to minimise systemic side effects and improve biosafety. We believe that future tumour suppression strategies may increasingly utilise endogenous cellular components, particularly ions, as therapeutic effectors. Importantly, the diverse roles of ions in cellular metabolism should not be overlooked.

While some studies have begun to explore metabolic pathways as targets for ion interference, this strategy remains relatively underexplored compared with other emerging modalities such as immunotherapy and gene editing. From a translational perspective, ion interference offers several distinctive features compared with established clinical treatments. Unlike conventional chemotherapy, which often relies on systemic drug exposure, ion-based strategies can exploit tumour-specific microenvironments (e.g., acidity, redox imbalance) to achieve more localised and responsive effects. Compared with radiotherapy, which induces damage through external energy input, ion interference operates through intracellular biochemical disruption. These characteristics highlight the unique potential of ion interference as a complementary therapeutic strategy.

To fully realise the potential of ion interference therapy, future research should focus on several key areas. First, the development of multifunctional ion-based systems integrating imaging, drug delivery, and therapeutic functions will be important for improving treatment specificity and efficacy. In addition, the integration of stimulus-responsive nanocarriers and bio-inspired delivery systems, such as exosomes, holds considerable promise for enhancing targeting capability. Second, deeper mechanistic understanding is required, particularly regarding ion-regulated metabolic pathways and



signalling cascades. Third, the roles of ions beyond tumour cells should be further explored, including their effects on the immune system, intercellular communication, and the tumour microenvironment.

In summary, ion interference represents a promising and versatile strategy in the evolving landscape of cancer treatment. By integrating advances in nanotechnology with a deeper understanding of ion-regulated biological processes, nano-enabled ion interference strategies are expected to play an increasingly important role in the development of next-generation precision therapies.

## Author contributions

Xinkai Hu: drafted and revised the manuscript and prepared the graphical illustrations. Dongdong Guo: contributed to the initial manuscript preparation. Nguyen T. K. Thanh: critically reviewed the manuscript.

## Conflicts of interest

There are no conflicts to declare

## Data availability

No primary research results, software or code have been included, and no new data were generated or analysed as part of this review.

## Acknowledgements

Xinkai Hu gratefully acknowledges financial support from the China Scholarship Council–UCL Joint Research Scholarship. Dongdong Guo thanks for the UCL Studentship and the Guangzhou Elite Scholarship for their generous support.

## References

- Wang, X.; Zhong, X.; Liu, Z.; Cheng, L. Recent progress of chemodynamic therapy-induced combination cancer therapy. *Nano Today* 2020, 35. DOI: 10.1016/j.nantod.2020.100946.
- Mishchenko, T. A.; Balalaeva, I. V.; Vedunova, M. V.; Krysko, D. V. Ferroptosis and Photodynamic Therapy Synergism: Enhancing Anticancer Treatment. *Trends Cancer* 2021, 7 (6), 484–487. DOI: 10.1016/j.trecan.2021.01.013.
- Huang, X.; Lu, Y.; Guo, M.; Du, S.; Han, N. Recent strategies for nano-based PTT combined with immunotherapy: from a biomaterial point of view. *Theranostics* 2021, 11 (15), 7546–7569. DOI: 10.7150/thno.56482.
- Qian, X.; Zheng, Y.; Chen, Y. Micro/Nanoparticle-Augmented Sonodynamic Therapy (SDT): Breaking the Depth Shallow of Photoactivation. *Adv Mater* 2016, 28 (37), 8097–8129. DOI: 10.1002/adma.201602012.
- Liu, M.; Anderson, R. C.; Lan, X.; Conti, P. S.; Chen, K. Recent advances in the development of nanoparticles for multimodality imaging and therapy of cancer. *Med Res Rev* 2020, 40 (3), 909–930. DOI: 10.1002/med.21642.
- Wu, J. L. Y.; Ji, Q.; Blackadar, C.; Nguyen, L. N. M.; Lin, Z. P.; Sepahi, Z.; Stordy, B. P.; Granda Farias, A.; Sindhvani, S.; Ngo, W.; et al. The pathways for nanoparticle transport across tumour endothelium. *Nat Nanotechnol* 2025, 20 (5), 672–682. DOI: 10.1038/s41565-025-01877-5 From NLM.
- Nguyen, B. L.; Le, N. D.; Nguyen, T. O. O.; Ahn, D.; Patil, B. R.; Kim, B.; Phung, C. D.; Pham, D.-V.; Lee, J. M.; Hong, J.; et al. Binary mineral nanoparticles enable intravascular delivery of metal ions to tumors for metalloimmunotherapy. *Nature Communications* 2026, 17 (1), 1556. DOI: 10.1038/s41467-025-68279-y.
- Ji, X.; Zhou, Y.; Li, Q.; Song, H.; Fan, C. Protein-Mimicking Nanoparticles for a Cellular Regulation of Homeostasis. *ACS Appl Mater Interfaces* 2021, 13 (27), 31331–31336. DOI: 10.1021/acsami.1c09281.
- Lerner, M. I.; Mikhaylov, G.; Tsukanov, A. A.; Lozhkomoev, A. S.; Gutmanas, E.; Gotman, I.; Bratovs, A.; Turk, V.; Turk, B.; Psakhye, S. G.; et al. Crumpled Aluminum Hydroxide Nanostructures as a Microenvironment Dysregulation Agent for Cancer Treatment. *Nano Lett* 2018, 18 (9), 5401–5410. DOI: 10.1021/acs.nanolett.8b01592.
- Storm, P.; Klausen, T. K.; Trulsson, M.; Ho, C. S. J.; Dosnon, M.; Westergren, T.; Chao, Y.; Rydstrom, A.; Yang, H.; Pedersen, S. F.; et al. A unifying mechanism for cancer cell death through ion channel activation by HAMLET. *PLoS One* 2013, 8 (3), e58578. DOI: 10.1371/journal.pone.0058578.
- Shen, Z.; Liu, T.; Li, Y.; Lau, J.; Yang, Z.; Fan, W.; Zhou, Z.; Shi, C.; Ke, C.; Bregadze, V. I.; et al. Fenton-Reaction-Acceleratable Magnetic Nanoparticles for Ferroptosis Therapy of Orthotopic Brain Tumors. *ACS Nano* 2018, 12 (11), 11355–11365. DOI: 10.1021/acs.nano.8b06201.
- Xu, Y.; Guo, Y.; Zhang, C.; Zhan, M.; Jia, L.; Song, S.; Jiang, C.; Shen, M.; Shi, X. Fibronectin-Coated Metal-Phenolic Networks for Cooperative Tumor Chemo-/Chemodynamic/Immune Therapy via Enhanced Ferroptosis-Mediated Immunogenic Cell Death. *ACS Nano* 2022. DOI: 10.1021/acs.nano.1c08585.
- Li, F.; Song, N.; Dong, Y.; Li, S.; Li, L.; Liu, Y.; Li, Z.; Yang, D. A Proton-Activatable DNA-Based Nanosystem Enables Co-Delivery of CRISPR/Cas9 and DNAzyme for Combined Gene Therapy. *Angew Chem Int Ed Engl* 2022, e202116569. DOI: 10.1002/anie.202116569.
- Zhang, C.; Hu, J.; Jiang, Y.; Tan, S.; Zhu, K.; Xue, C.; Dai, Y.; Chen, F. Biomimetic-inspired synthesis of amorphous manganese phosphates for GLUT5-targeted drug-free catalytic therapy of osteosarcoma. *Nanoscale* 2022, 14 (3), 898–909. DOI: 10.1039/d1nr06220d.
- Hu, K.; Xie, L.; Zhang, Y.; Hanyu, M.; Yang, Z.; Nagatsu, K.; Suzuki, H.; Ouyang, J.; Ji, X.; Wei, J.; et al. Marriage of black phosphorus and Cu(2+) as effective photothermal agents for PET-guided combination cancer therapy. *Nat Commun* 2020, 11 (1), 2778. DOI: 10.1038/s41467-020-16513-0.
- Fu, L. H.; Wan, Y.; Qi, C.; He, J.; Li, C.; Yang, C.; Xu, H.; Lin, J.; Huang, P. Nanocatalytic Theranostics with Glutathione Depletion and Enhanced Reactive Oxygen Species Generation for Efficient Cancer Therapy. *Adv Mater* 2021, 33 (7), e2006892. DOI: 10.1002/adma.202006892.
- Chen, X.; Chen, Y.; Wang, C.; Jiang, Y.; Chu, X.; Wu, F.; Wu, Y.; Cai, X.; Cao, Y.; Liu, Y. NIR - Triggered Intracellular H<sup>+</sup> Transients for Lamellipodia - Collapsed Antimetastasis and Enhanced Chemodynamic Therapy. *Angewandte Chemie International Edition* 2021, 60 (40), 21905–21910.
- Wang, S.; Liu, X.; Chen, S.; Liu, Z.; Zhang, X.; Liang, X. J.; Li, L. Regulation of Ca(2+) Signaling for Drug-Resistant Breast Cancer Therapy with Mesoporous Silica Nanocapsule Encapsulated Doxorubicin/siRNA Cocktail. *ACS Nano* 2019, 13 (1), 274–283. DOI: 10.1021/acs.nano.8b05639.
- Chu, X.; Jiang, X.; Liu, Y.; Zhai, S.; Jiang, Y.; Chen, Y.; Wu, J.; Wang, Y.; Wu, Y.; Tao, X.; et al. Nitric Oxide Modulating Calcium Store for Ca<sup>2+</sup> Initiated Cancer Therapy. *Advanced*



- Functional Materials 2021, 31 (13). DOI: 10.1002/adfm.202008507.
- 20 Ghosh, P.; Maayan, G. A rationally designed peptoid for the selective chelation of Zn(2+) over Cu(2). *Chem Sci* 2020, 11 (37), 10127-10134. DOI: 10.1039/d0sc03391j.
- 21 Tan, L.; He, C.; Chu, X.; Chu, Y.; Ding, Y. Charge-reversal ZnO-based nanospheres for stimuli-responsive release of multiple agents towards synergistic cancer therapy. *Chemical Engineering Journal* 2020, 395. DOI: 10.1016/j.cej.2020.125177.
- 22 Taieb, H. M.; Garske, D. S.; Contzen, J.; Gossen, M.; Bertinetti, L.; Robinson, T.; Cipitria, A. Osmotic pressure modulates single cell cycle dynamics inducing reversible growth arrest and reactivation of human metastatic cells. *Sci Rep* 2021, 11 (1), 13455. DOI: 10.1038/s41598-021-92054-w.
- 23 Irianto, J.; Swift, J.; Martins, R. P.; McPhail, G. D.; Knight, M. M.; Discher, D. E.; Lee, D. A. Osmotic challenge drives rapid and reversible chromatin condensation in chondrocytes. *Biophys J* 2013, 104 (4), 759-769. DOI: 10.1016/j.bpj.2013.01.006.
- 24 Cox, C. D.; Bavi, N.; Martinac, B. Biophysical Principles of Ion-Channel-Mediated Mechanosensory Transduction. *Cell Rep* 2019, 29 (1), 1-12. DOI: 10.1016/j.celrep.2019.08.075.
- 25 Prevarskaya, N.; Skryma, R.; Shuba, Y. Ion channels and the hallmarks of cancer. *Trends Mol Med* 2010, 16 (3), 107-121. DOI: 10.1016/j.molmed.2010.01.005.
- 26 Alam Shibly, S. U.; Ghatak, C.; Sayem Karal, M. A.; Moniruzzaman, M.; Yamazaki, M. Experimental Estimation of Membrane Tension Induced by Osmotic Pressure. *Biophys J* 2016, 111 (10), 2190-2201. DOI: 10.1016/j.bpj.2016.09.043.
- 27 Kültz, D.; Burg, M. Evolution of osmotic stress signaling via MAP kinase cascades. *J Exp Biol* 1998, 201 (Pt 22), 3015-3021. DOI: 10.1242/jeb.201.22.3015 From NLM.
- 28 Ahmed, B.; Dwivedi, S.; Abidin, M. Z.; Azam, A.; Al-Shaeri, M.; Khan, M. S.; Saquib, Q.; Al-Khedhairi, A. A.; Musarrat, J. Mitochondrial and Chromosomal Damage Induced by Oxidative Stress in Zn(2+) Ions, ZnO-Bulk and ZnO-NPs treated Allium cepa roots. *Sci Rep* 2017, 7, 40685. DOI: 10.1038/srep40685.
- 29 Zhu, Y.; Li, W.; Zhang, Y.; Li, J.; Liang, L.; Zhang, X.; Chen, N.; Sun, Y.; Chen, W.; Tai, R.; et al. Excessive sodium ions delivered into cells by nanodiamonds: implications for tumor therapy. *Small* 2012, 8 (11), 1771-1779. DOI: 10.1002/sml.201102539.
- 30 Jain, A. K.; Thareja, S. In vitro and in vivo characterization of pharmaceutical nanocarriers used for drug delivery. *Artif Cells Nanomed Biotechnol* 2019, 47 (1), 524-539. DOI: 10.1080/21691401.2018.1561457.
- 31 Blanco, E.; Shen, H.; Ferrari, M. Principles of nanoparticle design for overcoming biological barriers to drug delivery. *Nat Biotechnol* 2015, 33 (9), 941-951. DOI: 10.1038/nbt.3330.
- 32 Zhu, Y.; Zhang, Y.; Shi, G.; Yang, J.; Zhang, J.; Li, W.; Li, A.; Tai, R.; Fang, H.; Fan, C.; et al. Nanodiamonds act as Trojan horse for intracellular delivery of metal ions to trigger cytotoxicity. *Part Fibre Toxicol* 2015, 12, 2. DOI: 10.1186/s12989-014-0075-z.
- 33 Nel, A. E.; Madler, L.; Velegol, D.; Xia, T.; Hoek, E. M.; Somasundaran, P.; Klaessig, F.; Castranova, V.; Thompson, M. Understanding biophysicochemical interactions at the nanobio interface. *Nat Mater* 2009, 8 (7), 543-557. DOI: 10.1038/nmat2442.
- 34 Bertrand, N.; Grenier, P.; Mahmoudi, M.; Lima, E. M.; Appel, E. A.; Dormont, F.; Lim, J. M.; Karnik, R.; Langer, R.; Farokhzad, O. C. Mechanistic understanding of in vivo protein corona formation on polymeric nanoparticles and impact on pharmacokinetics. *Nat Commun* 2017, 8 (1), 777. DOI: 10.1038/s41467-017-00600-w.
- 35 Jiang, W.; Yin, L.; Chen, H.; Paschall, A. V.; Zhang, L.; Fu, W.; Zhang, W.; Todd, T.; Yu, K. S.; Zhou, S.; et al. NaCl Nanoparticles as a Cancer Therapeutic. *Adv Mater* 2019, 31 (46), e1904058. DOI: 10.1002/adma.201904058.
- 36 Schwarz, E. C.; Qu, B.; Hoth, M. Calcium, cancer and killing: the role of calcium in killing cancer cells by cytotoxic T lymphocytes and natural killer cells. *Biochim Biophys Acta* 2013, 1833 (7), 1603-1611. DOI: 10.1016/j.bbamcr.2012.11.016.
- 37 Zhang, M.; Song, R.; Liu, Y.; Yi, Z.; Meng, X.; Zhang, J.; Tang, Z.; Yao, Z.; Liu, Y.; Liu, X.; et al. Calcium-Overload-Mediated Tumor Therapy by Calcium Peroxide Nanoparticles. *Chem* 2019, 5 (8), 2171-2182. DOI: 10.1016/j.chempr.2019.06.003.
- 38 Liu, C.; Cao, Y.; Cheng, Y.; Wang, D.; Xu, T.; Su, L.; Zhang, X.; Dong, H. An open source and reduce expenditure ROS generation strategy for chemodynamic/photodynamic synergistic therapy. *Nat Commun* 2020, 11 (1), 1735. DOI: 10.1038/s41467-020-15591-4.
- 39 Shen, J.; Yu, H.; Shu, Y.; Ma, M.; Chen, H. A Robust ROS Generation Strategy for Enhanced Chemodynamic/Photodynamic Therapy via H2O2/O2 Self-Supply and Ca2+ Overloading. *Advanced Functional Materials* 2021, 31 (50). DOI: 10.1002/adfm.202106106.
- 40 Yan, J.-H.; Meng, W.; Shan, H.; Zhang, X.-P.; Zou, L.-M.; Wang, L.-L.; Shi, J.-S.; Kong, X.-Y. Melanin Nanoparticles Combined with CaO2 Nanoparticles for Image-Guided Tumor Microenvironment-Responsive Multimodal Therapy. *ACS Applied Nano Materials* 2021, 4 (2), 1351-1363. DOI: 10.1021/acsanm.0c02916.
- 41 Chen, Q.; Huo, D.; Cheng, H.; Lyu, Z.; Zhu, C.; Guan, B.; Xia, Y. Near-Infrared-Triggered Release of Ca(2+) Ions for Potential Application in Combination Cancer Therapy. *Adv Healthc Mater* 2019, 8 (6), e1801113. DOI: 10.1002/adhm.201801113.
- 42 Pan, T.; Fu, W.; Xin, H.; Geng, S.; Li, Z.; Cui, H.; Zhang, Y.; Chu, P. K.; Zhou, W.; Yu, X. F. Calcium Phosphate Mineralized Black Phosphorous with Enhanced Functionality and Anticancer Bioactivity. *Advanced Functional Materials* 2020. DOI: 10.1002/adfm.202003069.
- 43 Li, Y.; Zhou, S.; Song, H.; Yu, T.; Zheng, X.; Chu, Q. CaCO3 nanoparticles incorporated with KAE to enable amplified calcium overload cancer therapy. *Biomaterials* 2021, 277, 121080. DOI: 10.1016/j.biomaterials.2021.121080.
- 44 Wang, C.; Yu, F.; Liu, X.; Chen, S.; Wu, R.; Zhao, R.; Hu, F.; Yuan, H. Cancer-Specific Therapy by Artificial Modulation of Intracellular Calcium Concentration. *Adv Healthc Mater* 2019, 8 (18), e1900501. DOI: 10.1002/adhm.201900501.
- 45 Liu, J.; Jin, Y.; Song, Z.; Xu, L.; Yang, Y.; Zhao, X.; Wang, B.; Liu, W.; Zhang, K.; Zhang, Z.; et al. Boosting tumor treatment by dredging the hurdles of chemodynamic therapy synergistic ion therapy. *Chemical Engineering Journal* 2021, 411. DOI: 10.1016/j.cej.2021.128440.
- 46 Chen, F.; Yang, B.; Xu, L.; Yang, J.; Li, J. A CaO2 @Tannic Acid-Fe(III) Nanoconjugate for Enhanced Chemodynamic Tumor Therapy. *ChemMedChem* 2021, 16 (14), 2278-2286. DOI: 10.1002/cmdc.202100108.
- 47 Kong, H.; Chu, Q.; Fang, C.; Cao, G.; Han, G.; Li, X. Cu-Ferrocene-Functionalized CaO2 Nanoparticles to Enable Tumor-Specific Synergistic Therapy with GSH Depletion and Calcium Overload. *Adv Sci (Weinh)* 2021, e2100241. DOI: 10.1002/advs.202100241.
- 48 Hu, H.; Yu, L.; Qian, X.; Chen, Y.; Chen, B.; Li, Y. Chemoreactive Nanotherapeutics by Metal Peroxide Based Nanomedicine. *Adv Sci (Weinh)* 2020, 8 (1), 2000494. DOI: 10.1002/advs.202000494.
- 49 He, J.; Fu, L. H.; Qi, C.; Lin, J.; Huang, P. Metal peroxides for cancer treatment. *Bioact Mater* 2021, 6 (9), 2698-2710. DOI: 10.1016/j.bioactmat.2021.01.026.



- 50 Wiesmann, N.; Klueker, M.; Demuth, P.; Brenner, W.; Tremel, W.; Brieger, J. Zinc overload mediated by zinc oxide nanoparticles as innovative anti-tumor agent. *J Trace Elem Med Biol* 2019, 51, 226-234. DOI: 10.1016/j.jtemb.2018.08.002.
- 51 Lin, L. S.; Wang, J. F.; Song, J.; Liu, Y.; Zhu, G.; Dai, Y.; Shen, Z.; Tian, R.; Song, J.; Wang, Z.; et al. Cooperation of endogenous and exogenous reactive oxygen species induced by zinc peroxide nanoparticles to enhance oxidative stress-based cancer therapy. *Theranostics* 2019, 9 (24), 7200-7209. DOI: 10.7150/thno.39831.
- 52 Tardito, S.; Bassanetti, I.; Bignardi, C.; Elviri, L.; Tegoni, M.; Mucchino, C.; Bussolati, O.; Franchi-Gazzola, R.; Marchio, L. Copper binding agents acting as copper ionophores lead to caspase inhibition and paraptotic cell death in human cancer cells. *J Am Chem Soc* 2011, 133 (16), 6235-6242. DOI: 10.1021/ja109413c.
- 53 Arnal, N.; de Alaniz, M. J.; Marra, C. A. Cytotoxic effects of copper overload on human-derived lung and liver cells in culture. *Biochim Biophys Acta* 2012, 1820 (7), 931-939. DOI: 10.1016/j.bbagen.2012.03.007.
- 54 Arif, H.; Sohail, A.; Farhan, M.; Rehman, A. A.; Ahmad, A.; Hadi, S. M. Flavonoids-induced redox cycling of copper ions leads to generation of reactive oxygen species: A potential role in cancer chemoprevention. *Int J Biol Macromol* 2018, 106, 569-578. DOI: 10.1016/j.ijbiomac.2017.08.049.
- 55 Li, Y. Copper homeostasis: Emerging target for cancer treatment. *IUBMB Life* 2020, 72 (9), 1900-1908. DOI: 10.1002/iub.2341.
- 56 Chandy, K. G.; Norton, R. S. Channelling potassium to fight cancer. *Nature* 2016, 537 (7621), 497-499. DOI: 10.1038/nature19467.
- 57 Merlot, A. M.; Kalinowski, D. S.; Richardson, D. R. Novel chelators for cancer treatment: where are we now? *Antioxid Redox Signal* 2013, 18 (8), 973-1006. DOI: 10.1089/ars.2012.4540 From NLM.
- 58 Cui, L.; Gouw, A. M.; LaGory, E. L.; Guo, S.; Attarwala, N.; Tang, Y.; Qi, J.; Chen, Y. S.; Gao, Z.; Casey, K. M.; et al. Mitochondrial copper depletion suppresses triple-negative breast cancer in mice. *Nat Biotechnol* 2021, 39 (3), 357-367. DOI: 10.1038/s41587-020-0707-9.
- 59 Shao, S.; Si, J.; Shen, Y. Copper as the Target for Anticancer Nanomedicine. *Advanced Therapeutics* 2019, 2 (5). DOI: 10.1002/adtp.201800147.
- 60 Shanbhag, V. C.; Gudekar, N.; Jasmer, K.; Papageorgiou, C.; Singh, K.; Petris, M. J. Copper metabolism as a unique vulnerability in cancer. *Biochim Biophys Acta Mol Cell Res* 2021, 1868 (2), 118893. DOI: 10.1016/j.bbamcr.2020.118893.
- 61 Shao, S.; Zhou, Q.; Si, J.; Tang, J.; Liu, X.; Wang, M.; Gao, J.; Wang, K.; Xu, R.; Shen, Y. A non-cytotoxic dendrimer with innate and potent anticancer and anti-metastatic activities. *Nat Biomed Eng* 2017, 1 (9), 745-757. DOI: 10.1038/s41551-017-0130-9.
- 62 Yang, J.; Yu, G.; Sessler, J. L.; Shin, I.; Gale, P. A.; Huang, F. Artificial transmembrane ion transporters as potential therapeutics. *Chem* 2021, 7 (12), 3256-3291. DOI: 10.1016/j.chempr.2021.10.028 (accessed 2026/04/01).
- 63 Lang, F.; Stourmaras, C. Ion channels in cancer: future perspectives and clinical potential. *Philos Trans R Soc Lond B Biol Sci* 2014, 369 (1638), 20130108. DOI: 10.1098/rstb.2013.0108.
- 64 Lee, J. M.; Davis, F. M.; Roberts-Thomson, S. J.; Monteith, G. R. Ion channels and transporters in cancer. 4. Remodeling of Ca(2+) signaling in tumorigenesis: role of Ca(2+) transport. *Am J Physiol Cell Physiol* 2011, 301 (5), C969-976. DOI: 10.1152/ajpcell.00136.2011.
- 65 Panyi, G.; Beeton, C.; Felipe, A. Ion channels and anti-cancer immunity. *Philos Trans R Soc Lond B Biol Sci* 2014, 369 (1638), 20130106. DOI: 10.1098/rstb.2013.0106.
- 66 Li, M.; Xiong, Z. G. Ion channels as targets for cancer therapy. *Int J Physiol Pathophysiol Pharmacol* 2011, 3 (2), 156-166. From NLM.
- 67 Leanza, L.; Manago, A.; Zoratti, M.; Gulbins, E.; Szabo, I. Pharmacological targeting of ion channels for cancer therapy: In vivo evidences. *Biochim Biophys Acta* 2016, 1863 (6 Pt B), 1385-1397. DOI: 10.1016/j.bbamcr.2015.11.032.
- 68 Panyi, G.; Vamosi, G.; Bodnar, A.; Gaspar, R.; Damjanovich, S. Looking through ion channels: recharged concepts in T-cell signaling. *Trends Immunol* 2004, 25 (11), 565-569. DOI: 10.1016/j.it.2004.09.002.
- 69 Djamgoz, M. B.; Coombes, R. C.; Schwab, A. Ion transport and cancer: from initiation to metastasis. *Philos Trans R Soc Lond B Biol Sci* 2014, 369 (1638), 20130092. DOI: 10.1098/rstb.2013.0092.
- 70 Prevarskaya, N.; Skryma, R.; Bidaux, G.; Flourakis, M.; Shuba, Y. Ion channels in death and differentiation of prostate cancer cells. *Cell Death Differ* 2007, 14 (7), 1295-1304. DOI: 10.1038/sj.cdd.4402162.
- 71 Capatina, A. L.; Lagos, D.; Brackenbury, W. J. Targeting Ion Channels for Cancer Treatment: Current Progress and Future Challenges. *Rev Physiol Biochem Pharmacol* 2020. DOI: 10.1007/112\_2020\_46.
- 72 Malla, J. A.; Umesh, R. M.; Yousef, S.; Mane, S.; Sharma, S.; Lahiri, M.; Talukdar, P. A Glutathione Activatable Ion Channel Induces Apoptosis in Cancer Cells by Depleting Intracellular Glutathione Levels. *Angew Chem Int Ed Engl* 2020, 59 (20), 7944-7952. DOI: 10.1002/anie.202000961.
- 73 Han, X.; Xi, L.; Wang, H.; Huang, X.; Ma, X.; Han, Z.; Wu, P.; Ma, X.; Lu, Y.; Wang, G.; et al. The potassium ion channel opener NS1619 inhibits proliferation and induces apoptosis in A2780 ovarian cancer cells. *Biochem Biophys Res Commun* 2008, 375 (2), 205-209. DOI: 10.1016/j.bbrc.2008.07.161.
- 74 He, T.; Wang, H.; Wang, T.; Pang, G.; Zhang, Y.; Zhang, C.; Yu, P.; Chang, J. Sonogenetic nanosystem activated mechanosensitive ion channel to induce cell apoptosis for cancer immunotherapy. *Chemical Engineering Journal* 2021, 407, 127173. DOI: https://doi.org/10.1016/j.cej.2020.127173.
- 75 Cox, J. H.; Hussell, S.; Sondergaard, H.; Roepstorff, K.; Bui, J. V.; Deer, J. R.; Zhang, J.; Li, Z. G.; Lamberth, K.; Kvist, P. H.; et al. Antibody-mediated targeting of the Orai1 calcium channel inhibits T cell function. *PLoS One* 2013, 8 (12), e82944. DOI: 10.1371/journal.pone.0082944.
- 76 Duranti, C.; Arcangeli, A. Ion Channel Targeting with Antibodies and Antibody Fragments for Cancer Diagnosis. *Antibodies (Basel)* 2019, 8 (2). DOI: 10.3390/antib8020033.
- 77 Monteith, G. R.; Davis, F. M.; Roberts-Thomson, S. J. Calcium channels and pumps in cancer: changes and consequences. *J Biol Chem* 2012, 287 (38), 31666-31673. DOI: 10.1074/jbc.R112.343061.
- 78 Monteith, G. R.; McAndrew, D.; Faddy, H. M.; Roberts-Thomson, S. J. Calcium and cancer: targeting Ca<sup>2+</sup> transport. *Nat Rev Cancer* 2007, 7 (7), 519-530. DOI: 10.1038/nrc2171.
- 79 Huang, X.; Jan, L. Y. Targeting potassium channels in cancer. *J Cell Biol* 2014, 206 (2), 151-162. DOI: 10.1083/jcb.201404136.
- 80 Fong, C. W. Platinum anti-cancer drugs: Free radical mechanism of Pt-DNA adduct formation and anti-neoplastic effect. *Free Radic Biol Med* 2016, 95, 216-229. DOI: 10.1016/j.freeradbiomed.2016.03.006.
- 81 Dasari, S.; Tchounwou, P. B. Cisplatin in cancer therapy: molecular mechanisms of action. *Eur J Pharmacol* 2014, 740, 364-378. DOI: 10.1016/j.ejphar.2014.07.025.
- 82 Dhar, S.; Gu, F. X.; Langer, R.; Farokhzad, O. C.; Lippard, S. J. Targeted delivery of cisplatin to prostate cancer cells by



- aptamer functionalized Pt(IV) prodrug-PLGA-PEG nanoparticles. *Proc Natl Acad Sci U S A* 2008, 105 (45), 17356-17361. DOI: 10.1073/pnas.0809154105.
- 83 Badeau, B. A.; DeForest, C. A. Programming Stimuli-Responsive Behavior into Biomaterials. *Annu Rev Biomed Eng* 2019, 21, 241-265. DOI: 10.1146/annurev-bioeng-060418-052324.
- 84 Browning, R. J.; Reardon, P. J. T.; Parhizkar, M.; Pedley, R. B.; Edirisinghe, M.; Knowles, J. C.; Stride, E. Drug Delivery Strategies for Platinum-Based Chemotherapy. *ACS Nano* 2017, 11 (9), 8560-8578. DOI: 10.1021/acsnano.7b04092.
- 85 Michalke, B. Platinum speciation used for elucidating activation or inhibition of Pt-containing anti-cancer drugs. *J Trace Elem Med Biol* 2010, 24 (2), 69-77. DOI: 10.1016/j.jtemb.2010.01.006.
- 86 Aydin, A.; Korkmaz, N.; Tekin, S.; Karadağ, A. Anticancer activities and mechanism of action of 2 novel metal complexes, C16H34N8O5Ag2Cd and C11H16N7O2Ag3Ni. *Turkish Journal of Biology* 2014, 38, 948-955. DOI: 10.3906/biy-1405-68.
- 87 AshaRani, P. V.; Low Kah Mun, G.; Hande, M. P.; Valiyaveetil, S. Cytotoxicity and Genotoxicity of Silver Nanoparticles in Human Cells. *ACS Nano* 2009, 3 (2), 279-290. DOI: 10.1021/nn800596w.
- 88 Foldbjerg, R.; Dang, D. A.; Autrup, H. Cytotoxicity and genotoxicity of silver nanoparticles in the human lung cancer cell line, A549. *Arch Toxicol* 2011, 85 (7), 743-750. DOI: 10.1007/s00204-010-0545-5.
- 89 Wei, L.; Lu, J.; Xu, H.; Patel, A.; Chen, Z. S.; Chen, G. Silver nanoparticles: synthesis, properties, and therapeutic applications. *Drug Discov Today* 2015, 20 (5), 595-601. DOI: 10.1016/j.drudis.2014.11.014.
- 90 Lin, J.; Huang, Z.; Wu, H.; Zhou, W.; Jin, P.; Wei, P.; Zhang, Y.; Zheng, F.; Zhang, J.; Xu, J.; et al. Inhibition of autophagy enhances the anticancer activity of silver nanoparticles. *Autophagy* 2014, 10 (11), 2006-2020. DOI: 10.4161/auto.36293.
- 91 Ceramella, J.; Mariconda, A.; Iacopetta, D.; Saturnino, C.; Barbarossa, A.; Caruso, A.; Rosano, C.; Sinicropi, M. S.; Longo, P. From coins to cancer therapy: Gold, silver and copper complexes targeting human topoisomerases. *Bioorg Med Chem Lett* 2020, 30 (3), 126905. DOI: 10.1016/j.bmcl.2019.126905.
- 92 Ivey, J. W.; Bonakdar, M.; Kanitkar, A.; Davalos, R. V.; Verbridge, S. S. Improving cancer therapies by targeting the physical and chemical hallmarks of the tumor microenvironment. *Cancer Lett* 2016, 380 (1), 330-339. DOI: 10.1016/j.canlet.2015.12.019.
- 93 Ranji-Burachaloo, H.; Gurr, P. A.; Dunstan, D. E.; Qiao, G. G. Cancer Treatment through Nanoparticle-Facilitated Fenton Reaction. *ACS Nano* 2018, 12 (12), 11819-11837. DOI: 10.1021/acsnano.8b07635.
- 94 Gao, L.; Zhuang, J.; Nie, L.; Zhang, J.; Zhang, Y.; Gu, N.; Wang, T.; Feng, J.; Yang, D.; Perrett, S.; et al. Intrinsic peroxidase-like activity of ferromagnetic nanoparticles. *Nat Nanotechnol* 2007, 2 (9), 577-583. DOI: 10.1038/nnano.2007.260.
- 95 Li, W. P.; Su, C. H.; Chang, Y. C.; Lin, Y. J.; Yeh, C. S. Ultrasound-Induced Reactive Oxygen Species Mediated Therapy and Imaging Using a Fenton Reaction Activable Polymersome. *ACS Nano* 2016, 10 (2), 2017-2027. DOI: 10.1021/acsnano.5b06175.
- 96 Yang, J.; Ma, S.; Xu, R.; Wei, Y.; Zhang, J.; Zuo, T.; Wang, Z.; Deng, H.; Yang, N.; Shen, Q. Smart biomimetic metal organic frameworks based on ROS-ferroptosis-glycolysis regulation for enhanced tumor chemo-immunotherapy. *J Control Release* 2021, 334, 21-33. DOI: 10.1016/j.jconrel.2021.04.013.
- 97 Meng, X.; Zhang, F.; Guo, H.; Zhang, C.; Hu, H.; Wang, W.; Liu, J.; Shuai, X.; Cao, Z. One - Pot Approach to Fe<sub>2+</sub>/Fe<sub>3+</sub> Based MOFs with Enhanced Catalytic Activity for Fenton Reaction. *Advanced Healthcare Materials* 2021, 2100780. DOI: 10.1002/adhm.202100780
- 98 Jia, T.; Wang, Z.; Sun, Q.; Dong, S.; Xu, J.; Zhang, F.; Feng, L.; He, F.; Yang, D.; Yang, P.; et al. Intelligent Fe-Mn Layered Double Hydroxides Nanosheets Anchored with Upconversion Nanoparticles for Oxygen-Elevated Synergetic Therapy and Bioimaging. *Small* 2020, 16 (46), e2001343. DOI: 10.1002/smll.202001343.
- 99 Liang, H.; Guo, J.; Shi, Y.; Zhao, G.; Sun, S.; Sun, X. Porous yolk-shell Fe/Fe<sub>3</sub>O<sub>4</sub> nanoparticles with controlled exposure of highly active Fe (0) for cancer therapy. *Biomaterials* 2021, 268, 120530. DOI: 10.1016/j.biomaterials.2020.120530.
- 100 Ding, T.; Wang, Z.; Xia, D.; Zhu, J.; Huang, J.; Xing, Y.; Wang, S.; Chen, Y.; Zhang, J.; Cai, K. Long - Lasting Reactive Oxygen Species Generation by Porous Redox Mediator - Potentiated Nanoreactor for Effective Tumor Therapy. *Advanced Functional Materials* 2021, 31 (13). DOI: 10.1002/adfm.202008573.
- 101 Liu, Y.; Wang, Y.; Song, S.; Zhang, H. Cascade-responsive nanobomb with domino effect for anti-tumor synergistic therapies. *National Science Review* 2022, 9 (3), nwab139. DOI: 10.1093/nsr/nwab139 (accessed 3/27/2025).
- 102 Su, Y.; Cockerill, I.; Wang, Y.; Qin, Y. X.; Chang, L.; Zheng, Y.; Zhu, D. Zinc-Based Biomaterials for Regeneration and Therapy. *Trends Biotechnol* 2019, 37 (4), 428-441. DOI: 10.1016/j.tibtech.2018.10.009.
- 103 Wang, J.; Zhao, H.; Xu, Z.; Cheng, X. Zinc dysregulation in cancers and its potential as a therapeutic target. *Cancer Biol Med* 2020, 17 (3), 612-625. DOI: 10.20892/j.issn.2095-3941.2020.0106.
- 104 Ruan, J.; Qian, H. Recent Development on Controlled Synthesis of Mn - Based Nanostructures for Bioimaging and Cancer Therapy. *Advanced Therapeutics* 2021, 4 (5). DOI: 10.1002/adtp.202100018.
- 105 Fu, L. H.; Hu, Y. R.; Qi, C.; He, T.; Jiang, S.; Jiang, C.; He, J.; Qu, J.; Lin, J.; Huang, P. Biodegradable Manganese-Doped Calcium Phosphate Nanotheranostics for Traceable Cascade Reaction-Enhanced Anti-Tumor Therapy. *ACS Nano* 2019, 13 (12), 13985-13994. DOI: 10.1021/acsnano.9b05836.
- 106 Niu, B.; Liao, K.; Zhou, Y.; Wen, T.; Quan, G.; Pan, X.; Wu, C. Application of glutathione depletion in cancer therapy: Enhanced ROS-based therapy, ferroptosis, and chemotherapy. *Biomaterials* 2021, 277, 121110. DOI: 10.1016/j.biomaterials.2021.121110.
- 107 Lu, Z.; Gao, J.; Fang, C.; Zhou, Y.; Li, X.; Han, G. Porous Pt Nanospheres Incorporated with GOx to Enable Synergistic Oxygen - Inductive Starvation/Electrodynamical Tumor Therapy. *Advanced Science* 2020, 7 (17), 2001223.
- 108 Zhang, Y.; Yang, Y.; Jiang, S.; Li, F.; Lin, J.; Wang, T.; Huang, P. Degradable silver-based nanoplatform for synergistic cancer starving-like/metal ion therapy. *Materials Horizons* 2019, 6 (1), 169-175. DOI: 10.1039/c8mh00908b.
- 109 Zhang, X.; He, C.; Chen, Y.; Chen, C.; Yan, R.; Fan, T.; Gai, Y.; Yang, T.; Lu, Y.; Xiang, G. Cyclic reactions-mediated self-supply of H<sub>2</sub>O<sub>2</sub> and O<sub>2</sub> for cooperative chemodynamic/starvation cancer therapy. *Biomaterials* 2021, 120987.
- 110 Yang, B.; Ding, L.; Chen, Y.; Shi, J. Augmenting Tumor-Starvation Therapy by Cancer Cell Autophagy Inhibition. *Adv Sci (Weinh)* 2020, 7 (6), 1902847. DOI: 10.1002/advs.201902847.
- 111 Sun, X.; James, T. D. Glucose Sensing in Supramolecular Chemistry. *Chem Rev* 2015, 115 (15), 8001-8037. DOI: 10.1021/cr500562m.



- 112 Chen, L.; Cui, H. Targeting Glutamine Induces Apoptosis: A Cancer Therapy Approach. *Int J Mol Sci* 2015, 16 (9), 22830-22855. DOI: 10.3390/ijms160922830.
- 113 Cluntun, A. A.; Lukey, M. J.; Cerione, R. A.; Locasale, J. W. Glutamine Metabolism in Cancer: Understanding the Heterogeneity. *Trends Cancer* 2017, 3 (3), 169-180. DOI: 10.1016/j.trecan.2017.01.005.
- 114 Leone, R. D.; Zhao, L.; Englert, J. M.; Sun, I. M.; Oh, M. H.; Sun, I. H.; Arwood, M. L.; Bettencourt, I. A.; Patel, C. H.; Wen, J.; et al. Glutamine blockade induces divergent metabolic programs to overcome tumor immune evasion. *Science* 2019, 366 (6468), 1013-1021. DOI: 10.1126/science.aav2588 From NLM.
- 115 Zhang, C.; Ni, D.; Liu, Y.; Yao, H.; Bu, W.; Shi, J. Magnesium silicide nanoparticles as a deoxygenation agent for cancer starvation therapy. *Nature Nanotechnology* 2017, 12 (4), 378-386. DOI: 10.1038/nnano.2016.280.
- 116 Zhang, R.; Feng, L.; Dong, Z.; Wang, L.; Liang, C.; Chen, J.; Ma, Q.; Zhang, R.; Chen, Q.; Wang, Y.; et al. Glucose & oxygen exhausting liposomes for combined cancer starvation and hypoxia-activated therapy. *Biomaterials* 2018, 162, 123-131. DOI: 10.1016/j.biomaterials.2018.02.004.
- 117 Yang, Y.; Lu, Y.; Abbaraju, P. L.; Azimi, I.; Lei, C.; Tang, J.; Jambhrunkar, M.; Fu, J.; Zhang, M.; Liu, Y.; et al. Stepwise Degradable Nanocarriers Enabled Cascade Delivery for Synergistic Cancer Therapy. *Advanced Functional Materials* 2018, 28 (28). DOI: 10.1002/adfm.201800706.
- 118 Liu, G.; Zhu, J.; Guo, H.; Sun, A.; Chen, P.; Xi, L.; Huang, W.; Song, X.; Dong, X. Mo<sub>2</sub> C-Derived Polyoxometalate for NIR-II Photoacoustic Imaging-Guided Chemodynamic/Photothermal Synergistic Therapy. *Angew Chem Int Ed Engl* 2019, 58 (51), 18641-18646. DOI: 10.1002/anie.201910815.
- 119 Qiu, M.; Ren, W. X.; Jeong, T.; Won, M.; Park, G. Y.; Sang, D. K.; Liu, L. P.; Zhang, H.; Kim, J. S. Omnipotent phosphorene: a next-generation, two-dimensional nanoplatfor for multidisciplinary biomedical applications. *Chem Soc Rev* 2018, 47 (15), 5588-5601. DOI: 10.1039/c8cs00342d.
- 120 Wu, Y.; Song, X.; Xu, W.; Sun, K. Y.; Wang, Z.; Lv, Z.; Wang, Y.; Wang, Y.; Zhong, W.; Wei, J.; et al. NIR-Activated Multimodal Photothermal/Chemodynamic/Magnetic Resonance Imaging Nanoplatfor for Anticancer Therapy by Fe(II) Ions Doped MXenes (Fe-Ti<sub>3</sub> C<sub>2</sub>). *Small* 2021, 17 (33), e2101705. DOI: 10.1002/sml.202101705.
- 121 Li, S. L.; Jiang, P.; Jiang, F. L.; Liu, Y. Recent Advances in Nanomaterial - Based Nanoplatfor for Chemodynamic Cancer Therapy. *Advanced Functional Materials* 2021, 31 (22). DOI: 10.1002/adfm.202100243.
- 122 Sun, K.; Hu, J.; Meng, X.; Lei, Y.; Zhang, X.; Lu, Z.; Zhang, L.; Wang, Z. Reinforcing the Induction of Immunogenic Cell Death Via Artificial Engineered Cascade Bioreactor - Enhanced Chemo - Immunotherapy for Optimizing Cancer Immunotherapy. *Small* 2021, 17 (37), 2101897. DOI: 10.1002/sml.202101897.
- 123 Gu, Z.; Liu, T.; Liu, C.; Yang, Y.; Tang, J.; Song, H.; Wang, Y.; Yang, Y.; Yu, C. Ferroptosis-Strengthened Metabolic and Inflammatory Regulation of Tumor-Associated Macrophages Provokes Potent Tumorcidal Activities. *Nano Lett* 2021, 21 (15), 6471-6479. DOI: 10.1021/acs.nanolett.1c01401.
- 124 Wang, Z.; Liu, B.; Sun, Q.; Feng, L.; He, F.; Yang, P.; Gai, S.; Quan, Z.; Lin, J. Upconverted Metal-Organic Framework Janus Architecture for Near-Infrared and Ultrasound Co-Enhanced High Performance Tumor Therapy. *ACS Nano* 2021. DOI: 10.1021/acsnano.1c04280.
- 125 Tsai, M.-F.; Chang, S.-H. G.; Cheng, F.-Y.; Shanmugam, V.; Cheng, Y.-S.; Su, C.-H.; Yeh, C.-S. Au Nanorod Design as Light-Absorber in the First and Second Biological Near-Infrared Windows for in Vivo Photothermal Therapy. *ACS Nano* 2013, 7 (6), 5330-5342. DOI: 10.1021/nn401187c0130. view Article Online
- 126 Shi, X.-H.; Tao, L.; Wang, L.; Liu, X.; Liu, S.-L.; Wang, Z.-G. Plasmonic-Fluorescent Janus Au-PbS Nanoparticles with Bright Near-Infrared-IIb Fluorescence and Photothermal Effect for Computed Tomography Imaging-Guided Combination Cancer Therapy. *Chemistry of Materials* 2024, 36 (6), 2776-2789. DOI: 10.1021/acs.chemmater.3c02983.
- 127 Espinosa, A.; Reguera, J.; Curcio, A.; Muñoz-Noval, Á.; Kuttner, C.; Van de Walle, A.; Liz-Marzán, L. M.; Wilhelm, C. Janus Magnetic-Plasmonic Nanoparticles for Magnetically Guided and Thermally Activated Cancer Therapy. *Small* 2020, 16 (11), 1904960. DOI: https://doi.org/10.1002/sml.201904960.
- 128 Kim, D.; Jeong, Y. Y.; Jon, S. A Drug-Loaded Aptamer-Gold Nanoparticle Bioconjugate for Combined CT Imaging and Therapy of Prostate Cancer. *ACS Nano* 2010, 4 (7), 3689-3696. DOI: 10.1021/nn901877h.
- 129 Luo, Z.; Zheng, K.; Xie, J. Engineering ultrasmall water-soluble gold and silver nanoclusters for biomedical applications. *Chem Commun (Camb)* 2014, 50 (40), 5143-5155. DOI: 10.1039/c3cc47512c.
- 130 Singh, P.; Pandit, S.; Mokkalpati, V.; Garg, A.; Ravikumar, V.; Mijakovic, I. Gold Nanoparticles in Diagnostics and Therapeutics for Human Cancer. *Int J Mol Sci* 2018, 19 (7). DOI: 10.3390/ijms19071979.
- 131 Liu, M.; Li, Q.; Liang, L.; Li, J.; Wang, K.; Li, J.; Lv, M.; Chen, N.; Song, H.; Lee, J.; et al. Real-time visualization of clustering and intracellular transport of gold nanoparticles by correlative imaging. *Nat Commun* 2017, 8, 15646. DOI: 10.1038/ncomms15646.
- 132 Chen, W. H.; Luo, G. F.; Xu, X. D.; Jia, H. Z.; Lei, Q.; Han, K.; Zhang, X. Z. Cancer-targeted functional gold nanoparticles for apoptosis induction and real-time imaging based on FRET. *Nanoscale* 2014, 6 (16), 9531-9535. DOI: 10.1039/c4nr02516d.
- 133 Shin, T. H.; Kim, P. K.; Kang, S.; Cheong, J.; Kim, S.; Lim, Y.; Shin, W.; Jung, J. Y.; Lah, J. D.; Choi, B. W.; et al. High-resolution T1 MRI via renally clearable dextran nanoparticles with an iron oxide shell. *Nat Biomed Eng* 2021, 5 (3), 252-263. DOI: 10.1038/s41551-021-00687-z.
- 134 Besenhard, M. O.; Panariello, L.; Kiefer, C.; LaGrow, A. P.; Storozhuk, L.; Perton, F.; Begin, S.; Mertz, D.; Thanh, N. T. K.; Gavriilidis, A. Small iron oxide nanoparticles as MRI T1 contrast agent: scalable inexpensive water-based synthesis using a flow reactor. *Nanoscale* 2021, 13 (19), 8795-8805. DOI: 10.1039/d1nr00877c.
- 135 Bao, J.; Zu, X.; Wang, X.; Li, J.; Fan, D.; Shi, Y.; Xia, Q.; Cheng, J. Multifunctional Hf/Mn-TCPP Metal-Organic Framework Nanoparticles for Triple-Modality Imaging-Guided PTT/RT Synergistic Cancer Therapy. *International Journal of Nanomedicine* 2020, 15, 7687.
- 136 Lin, L. S.; Song, J.; Song, L.; Ke, K.; Liu, Y.; Zhou, Z.; Shen, Z.; Li, J.; Yang, Z.; Tang, W.; et al. Simultaneous Fenton-like Ion Delivery and Glutathione Depletion by MnO<sub>2</sub> -Based Nanoagent to Enhance Chemodynamic Therapy. *Angew Chem Int Ed Engl* 2018, 57 (18), 4902-4906. DOI: 10.1002/anie.201712027.
- 137 Zhang, M.; Shen, B.; Song, R.; Wang, H.; Lv, B.; Meng, X.; Liu, Y.; Liu, Y.; Zheng, X.; Su, W.; et al. Radiation-assisted metal ion interference tumor therapy by barium peroxide-based nanoparticles. *Materials Horizons* 2019, 6 (5), 1034-1040. DOI: 10.1039/c8mh01554f.
- 138 Dempsey, C.; Lee, I.; Cowan, K. R.; Suh, J. Coating barium titanate nanoparticles with polyethylenimine improves cellular uptake and allows for coupled imaging and gene delivery. *Colloids Surf B Biointerfaces* 2013, 112, 108-112. DOI: 10.1016/j.colsurfb.2013.07.045.



- 139 Chen, J.; Guo, Z.; Wang, H. B.; Gong, M.; Kong, X. K.; Xia, P.; Chen, Q. W. Multifunctional Fe<sub>3</sub>O<sub>4</sub>@C@Ag hybrid nanoparticles as dual modal imaging probes and near-infrared light-responsive drug delivery platform. *Biomaterials* 2013, 34 (2), 571-581. DOI: 10.1016/j.biomaterials.2012.10.002.
- 140 Zhong, D.; Zhao, J.; Li, Y.; Qiao, Y.; Wei, Q.; He, J.; Xie, T.; Li, W.; Zhou, M. Laser-triggered aggregated cubic alpha-Fe<sub>2</sub>O<sub>3</sub>@Au nanocomposites for magnetic resonance imaging and photothermal/enhanced radiation synergistic therapy. *Biomaterials* 2019, 219, 119369. DOI: 10.1016/j.biomaterials.2019.119369.
- 141 Wang, Y.; Li, Y.; Zhang, Z.; Wang, L.; Wang, D.; Tang, B. Z. Triple-Jump Photodynamic Theranostics: MnO<sub>2</sub> Combined Upconversion Nanoplatfoms Involving a Type-I Photosensitizer with Aggregation-Induced Emission Characteristics for Potent Cancer Treatment. *Adv Mater* 2021, e2103748. DOI: 10.1002/adma.202103748.
- 142 Tirukoti, N. D.; Avram, L.; Haris, T.; Lerner, B.; Diskin-Posner, Y.; Allouche-Arnon, H.; Bar-Shir, A. Fast Ion-Chelate Dissociation Rate for In Vivo MRI of Labile Zinc with Frequency-Specific Encodability. *J Am Chem Soc* 2021, 143 (30), 11751-11758. DOI: 10.1021/jacs.1c05376.
- 143 Yuan, Y.; Wei, Z.; Chu, C.; Zhang, J.; Song, X.; Walczak, P.; Bulte, J. W. M. Development of Zinc-Specific iCEST MRI as an Imaging Biomarker for Prostate Cancer. *Angew Chem Int Ed Engl* 2019, 58 (43), 15512-15517. DOI: 10.1002/anie.201909429.
- 144 Xu, J.; Shi, R.; Chen, G.; Dong, S.; Yang, P.; Zhang, Z.; Niu, N.; Gai, S.; He, F.; Fu, Y.; et al. All-in-One Theranostic Nanomedicine with Ultrabright Second Near-Infrared Emission for Tumor-Modulated Bioimaging and Chemodynamic/Photodynamic Therapy. *ACS Nano* 2020, 14 (8), 9613-9625. DOI: 10.1021/acsnano.0c00082.
- 145 Liu, L.; Wang, S.; Zhao, B.; Pei, P.; Fan, Y.; Li, X.; Zhang, F. Er(3+) Sensitized 1530 nm to 1180 nm Second Near-Infrared Window Upconversion Nanocrystals for In Vivo Biosensing. *Angew Chem Int Ed Engl* 2018, 57 (25), 7518-7522. DOI: 10.1002/anie.201802889.
- 146 Ren, F.; Ding, L.; Liu, H.; Huang, Q.; Zhang, H.; Zhang, L.; Zeng, J.; Sun, Q.; Li, Z.; Gao, M. Ultra-small nanocluster mediated synthesis of Nd(3+)-doped core-shell nanocrystals with emission in the second near-infrared window for multimodal imaging of tumor vasculature. *Biomaterials* 2018, 175, 30-43. DOI: 10.1016/j.biomaterials.2018.05.021.

View Article Online  
DOI: 10.1039/D5NR04488J



**Data availability statement**

No primary research results, software or code have been included, and no new data were generated or analysed as part of this review.

[View Article Online](#)

DOI: 10.1039/D5NR04488J

